A THESIS

FOR THE DEGREE OF MASTER OF SCIENCE

COMPREHENSIVE CHARACTERIZATION OF THREE GLUTATHIONE S-TRANSFERASE FAMILY PROTEINS (GST ω, GST ρ AND GST θ) FROM BLACK ROCKFISH (*Sebastes schlegeli*)

Jayasinghage Don Handun Eranga Jayasinghe

Department of Marine Life Sciences

GRADUATE SCHOOL

JEJU NATIONAL UNIVERSITY

February 2016

COMPREHENSIVE CHARACTERIZATION OF THREE GLUTATHIONE S-TRANSFERASE FAMILY PROTEINS (GST ω, GST ρ AND GST θ) FROM BLACK ROCKFISH (*Sebastes schlegeli*)
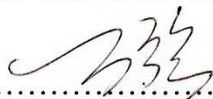
Jayasinghage Don Handun Eranga Jayasinghe

(Supervised by Professor Jehee Lee)

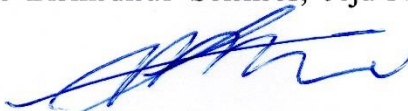A thesis submitted in partial fulfillment of the requirement for the degree of

MASTER OF SCIENCE

February 2016

This thesis has been examined and approved by

....

Thesis director, Qiang Wan (PhD), Research professor of Marine Life Sciences,

School of Marine Biomedical Sciences, Jeju National University

....

Chulhong Oh (PhD), Associate Professor of Marine Biology,

Korean Institute of Ocean Science & technology, University of Science & Technology

....

Jehee Lee (PhD), Professor of Marine Life Sciences,

School of Marine Biomedical Sciences, Jeju National University

Date : ....

Department of Marine Life Sciences

GRADUATE SCHOOL

JEJU NATIONAL UNIVERSITY

REPUBLIC OF KOREA

CONTENTS

ii

요 약 문

Glutathione-S-transferases (GSTs) 는 매우 다양한 촉매활성을 가지며 여러방면으로 중요한 기능을 수행하는 phase II enzymes에 속한다. 구핵성의 성향을 가지고 있는 GSTs는 글루타티온 (GSH) 을 음이온의 형태인 티올레트 형태 (GS-) 로 바꾸고 전자친화성 생체이물을 티올레이트와 복합체를 형성하는 반응을 촉진시킨다. GSTs는 다양한 전사와 전사후 변형을 통하여 특정 생체이물에 대한 내성을 조절하는 능력을 갖는데 이러한 GSTs의 해독능력은 마약류, 항생물질, 살충제 그리고 농약 개발에서 중요한 요소로서 알려져왔었다. Cytosolic GST인 GST omega (GSTω) 는 n-말단 연장선상에 Proline (19-20 residues) 이 풍부하고, GSH와 이황화 결합하는 활성부위에서 독특한 시스테인 잔기를 소유하고 있으며 이 부분에서 다른 GSTs들과 뚜렷하게 차이가 보인다. 또 다른 cytosolic GST인 GST rho (GSTρ)는 많은 연구에서 어류에서만 발견되는 GST로 밝혀져왔었지만, 최근 연체동물에서도 발견되었다고 보고되었다. Theta class GST (GSTθ) 는 또 다른 cytosolic GST로서 alpha, mu, Pi GST 등 다른 GST들과 구조뿐만 아니라 기능적으로도 다른 형태를 가지고 있다. GSTθ는 N-말단에 티로신 대신 세린잔기가 존재하며, 기질 1-chloro-2,4-dinitrobenzene (CDNB)에 반응하여 거의 검출되지 않을 정도의 극미량으로 활성을 띈다. 현재, 경골어류에서의 GSTω, GSTρ, GSTθ에 대한 연구가 미미한 실정이다.

본 연구에서는 조피볼락(*Sebastes schlegeli*)으로부터 GST계열의 3가지 paralogs (GSTω, GSTρ, GSTθ)를 이미 확립된 cDNA 데이터베이스와 NCBI-BLAST 도구를 이용하여 확인하였고, 분자적 특징은 molecular biological software and web-based servers 이용하였다. 생체이물 스트레스로부터 보호하기 위해 발생하는 항산화 정도와 생화학적 특성을 조사하기 위해 3개의 GST를 각각 pMAL-c5X vector에

클로닝하였고, Escherichia coli ER2523 cells에 형질 전환하여 다양한 assay를 실시하였다. 재조합 단백질은 과발현시켜 정제하였고, 다양한 기질에 대해 글루타티온 (GST) 을 감소시키는 활성을 조사하기 위해 분광광도분석을 실시하였다. 각 기질에 대해 온도별(10 °C – 60 °C) 과 pH별(3 – 12 pH) 의 영향에 따른 효능 평가를 수행하였고, Michaelis–Menten constant (Km)와 maximum reaction velocity (Vmax)를 조사하기 위해 Kinetic assays을 실시하였다. 상업적으로 이용가능한 두 개의 GST 억제제인 cibacron blue (CB) (0.001–100 μM)와 hematin (0.001–100 μM)를 사용하여 억제제의 영향에 대한 GST 촉매활성을 연구하고자 사용하였다. 또한, H2O2와 중금속 (Cd, Zn, Cu) 에 의해 발생되는 산화스트레스에 대한 생존효능을 측정하기 위해 디스크확산법을 실시하였다. 뿐만 아니라, 박테리아와 바이러스 자극제에 대한 반응을 보기 위해 조피볼락에 살아있는 *Streptococcus iniae* 박테리아와 polyinosinic:polycytidylic acid (poly I:C)를 접종하여 공격실험을 실시하였다. 공격실험 후, quantitative real time PCR (qPCR)을 이용하여 세 GST 유전자의 시간별 mRNA 발현양상을 조사하였다.

세 개의 GST 유전자는 모두 일반적인 도메인 구조를 가지고 있으며, 활성, 활성모티브, GSH binding pocket 구조에 따라 조금씩 구별되었다. 각 GST의 효소활성은 두 개의 기질을 통한 활성과 온도별, pH별 활성, 동력학적 계수를 통한 활성과 GST 억제제에 대한 실험을 통해 잠재적 억제 효능에 따라 각각의 GST는 서로 다른 활성을 나타내었고 이에 따른 기능적 차이를 보였다. 또한, 디스크 확산법은 통해 in vitro상에서 세 GST가 산화적 스트레스와 Cd, Cu, Zn 와 같은 중금속으로부터 보호해주는 것을 확인하였다. 세 유전자는 모두 면역 관련 조직에서 높은 발현을 보이고 있으며, 병원체 스트레스로 인한 RfGSTω와 RfGSTθ의 mRNA발

현 증가는 GST가 초기면역에 활발히 관여하고 있음을 보여준다. 종합해보면, 이 연구 결과는 경골어류로부터 GSTω, GSTρ, GSTθ 의 폭넓은 활성 범위를 보여주고 있으며 앞으로의 연구에 기반이 될 수 있을 것으로 보인다.

SUMMARY

GSTs are coming under the phase II enzymes which are an important multifunctional family accompanied with a wide variety of catalytic activities. GSTs catalyze the reduced glutathione (GSH) to form thiolate (GS⁻), the anion and form a complex with GST which nucleophilically attacks the close by electrophilic xenobiotics. GSTs undergo different transcriptional and posttranscriptional modifications and gain the ability to modulate resistance to specific xenobiotics. Due to their role in detoxification, GSTs have been identified as an important category in development of drugs, antibiotics, insecticides and pesticides. A cytosolic GST, GST omega (GSTω) distinctly differs from the other GSTs with the presence of N-terminal extension rich in Proline (19-20 residues) and possessing a unique cysteine residue at the active sites that can form a disulfide bond with GSH. GST rho (GSTρ), a cytosolic GST, has been identified as a fish specific GST in numerous studies but, recently it has been reported to be present in mollusks as well. Theta class GST (GSTθ), another cytosolic GST which is different from the other related GSTs such as Alpha, Mu and Pi class not only in struc

ture but also in function. GSTθ demonstrated minute or non-detectable activity towards the model substrate of the GSTs; 1-chloro-2,4-dinitrobenzene (CDNB) and in the place of N-terminal tyrosine, GSTθ possesses a serine residue. However, very limited reports are available in GSTω, GSTρ and GSTθ in accordance with teleosts.

In the present study, three paralogs of GST family; GSTω, GSTρ, and GSTθ from black rockfish (*Sebastes schlegeli*) was identified using a previously established cDNA database and with the help of NCBI-BLAST tool and molecularly characterized using molecular biological software and web-based servers. In order to investigate their biochemical characteristics and antioxidant dimensions to protect the fish from the xenobiotic stress, the three paralogs were independently cloned into pMAL-c5X vector, transformed into *Escherichia coli* ER2523 cells

and subjected to various assays. Recombinant proteins were over expressed and purified. Spectrophotometric analysis was carried out to determine the specific activities towards various substrates with reduced Glutathione (GSH). The effect of temperature (10 °C – 60 °C) and pH (3 – 12 pH) were assayed towards respective substrate. Kinetic assays were conducted to determine the Michaelis–Menten constant (K_m) and maximum reaction velocity (V_{max}). Two commercially available GST inhibitors cibacron blue (CB) (0.001–100 μM) and hematin (0.001–100 μM) were used to study the effect of inhibitors on the catalytic activity. Additionally, to determine the survival efficacy upon oxidative stress generated by H_2O_2 and heavy metals (Cd, Zn, Cu), disk diffusion assay was conducted. Furthermore, the response upon bacterial and viral stimuli, black rockfish were undergone challenge experiments with live *Streptococcus iniae* bacteria and polyinosinic:polycytidylic acid (poly I:C). The temporal transcriptional modulation of these three genes upon challenge experiments was investigated using quantitative real time PCR (qPCR).

The open reading frame (ORF) of *RfGSTω* was 717 bp and the putative protein encoded by the ORF was 239 amino acids in length and 28 kD in molecular weight. *RfGSTρ* consisted with an ORF of 678 bp and the putative protein was 226 amino acids in length with a molecular weight of 26 kD. Putative protein of *RfGSTθ* was 240 amino acids in length and 28 kD in molecular weight which was encoded by an ORF of 720 bp. The ExPASy prosite database revealed that the RfGSTω consisted of a GST N-terminal domain (Asn^{20} - Lys^{99}) where GST binding site (G-site) lies within and, a C-terminal domain (Ser^{104} - Val^{229}) where the substrate binding pocket (H-site) lies within. According to the results generated by the Pfam, the N-terminal domain of RfGSTρ was located at Gln^3 - Gly^{85} while C-terminal domain was located at Ser^{92} - Gln^{220}. In the instance of RfGSTθ, the N-terminal domain was lied at Met^1 - Asp^{80} while C-terminal domain was at Glu^{86} - Leu^{228}.

The ORFs of each three paralogs were cloned into pMAL-c5X expression vector,

respectively and overexpressed in *E. coli* ER2523. The fused proteins with maltose binding protein (MBP); rRfGSTω, rRfGSTρ and rRfGSTθ were purified separately and confirmed the purity using the SDS-PAGE analysis. The biochemical properties of each protein and MBP protein were analyzed using standard functional assays.

The rRfGSTω protein exhibited a detectable activity only towards DHA (0.36 ± 0.01 µmol min^{-1} mg^{-1}, n = 3), while both rRfGSTρ and rRfGSTθ showed detectable activities only towards CDNB (1.56 ± 0.01 µmol min^{-1} mg^{-1} and 2.05 ± 0.01 µmol min^{-1} mg^{-1}, n = 3). Subsequently, CDNB was selected as the respective substrate for both rRfGSTρ and rRfGSTθ while DHA was selected in the instance of rRfGSTω for further analysis. When the GSH concentration was fixed, the K_m and V_{max} values were 33.62 ± 2.05 mM and 18.04 ± 0.4 mM, respectively in the kinetic assay conducted with rRfGSTω where DHA was used as the substrate. For the same assay conducted with rRfGSTρ using CDNB as the substrate, the K_m and V_{max} values were 3.02 ± 0.08 mM and 3.40 ± 0.09 mM, respectively, while with rRfGSTθ the K_m and V_{max} values were 2.63 ± 0.04 mM and 15.80 ± 1.00 mM, respectively. The K_m and V_{max} values of rRfGSTω were 0.97 ± 0.14 mM and 2.02 ± 0.14 mM, respectively when the substrate concentration (DHA) was fixed. For the same assay conducted with CDNB as the substrate, the K_m and V_{max} values were 14.10 ± 0.25 mM and 11.28 ± 0.70 mM, respectively for rRfGSTρ, while with rRfGSTθ the K_m and V_{max} values were 1.40 ± 0.15 mM and 10.01 ± 0.75 mM, respectively.

The optimum temperature and the optimum pH for the DHAR activity with rRfGSTω were 40 °C and 8.5, respectively. Optimum temperatures for the CDNB conjugation activity with rRfGSTρ and rRfGSTθ were 40 °C and 20 °C, respectively while the optimum pH value was 7.5 in both of the instances. In the inhibition assay, the IC$_{50}$ (half maximal inhibitory concentration) values of the inhibition were 0.11 µM and 0.004 µM for CB and Hematin, respectively in the instance of rRfGSTω. In rRfGSTρ, the IC$_{50}$ values of the inhibition were 7

μM and 0.1 μM for CB and Hematin, respectively. In the instance of CDNB conjugation activity of rRfGSTθ, the IC_{50} values of the inhibition were 0.52 μM and 0.049 μM for CB and Hematin, respectively. Clearance zone was observed around the disks treated with 5 μL of H_2O_2 and the heavy metal treated disks in different magnitudes after incubation at 37 °C overnight. The rRfGSTω and rRfGSTθ transformed *E. coli* cells showed significance survival efficacy towards the oxidative stress developed by H_2O_2. All three genes implicated their protective potential towards the oxidative stress developed by heavy metals in different magnitudes.

All three paralogs (*RfGSTω*, *RfGSTρ* and *RfGSTθ*) were ubiquitously expressed in blood cells and all the tissues analyzed in the study namely; head kidney, spleen, liver, gill, intestine, kidney, heart, testis and ovary. The highest mRNA expression of *RfGSTω* was detected in blood, liver and ovary tissues. The *RfGSTρ* paralog was depicted its higher expression level in the liver, testes and ovary. Liver, testes and gill showed higher mRNA expression levels in the instance of *RfGSTθ*. Upon the *S. iniae* bacterial challenge, *RfGSTω* mRNA level in blood was significantly elevated at 3 hours post injection (h.p.i) and 6 h.p.i., respectively. *RfGSTρ* mRNA expression level in liver tissue was significantly down-regulated at the early phase of the bacterial infection and. Significant up-regulation of *RfGSTθ* mRNA expression in liver tissue was observed at all the time points except at 24 h.p.i. Poly I:C challenge experiment results revealed that, *RfGSTω* mRNA level could be significantly up-regulated by viral stimuli. The expression level of *RfGSTρ* mRNA in liver tissue showed a fluctuated pattern with significant down-regulations and control levels. *RfGSTθ* mRNA expression in liver tissue achieved its highest mRNA level at 48 h.p.i.

All three paralogs revealed their common domain architecture though they were slightly diverged from their corresponding orthologs in respect to activities, active moieties and GSH binding pocket architectures. Their enzymatic activities towards respective substrates, activities under different temperatures and pH values, kinetic parameters as well as inhibitory

potential generated by known GST inhibitors reveled their functional variation and validated their existence as paralogs. Additionally, the protective dimensions of three paralogs against oxidative stress and heavy metals such as Cd, Cu and Zn *in vitro* has been revealed. Since their mRNA expressional modulation appeared in higher magnitudes, it can be suggested that GST paralogs in this study are actively involved in innate immunity and the axiom was reinforced by the up-regulated expression of mRNA in respect to *RfGSTω* and *RfGSTθ* paralogs under pathogenic stress. Collectively, these findings deliver the broadened scopes of GSTω, GSTρ, and GSTθ paralogs from teleost species opening new dimensions for further studies.

LIST OF FIGURES

LIST OF TABLES

1. INTRODUCTION

Black rockfish or Korean rockfish, *Sebastes schlegeli* (Fig. 1), is a well-known sedentary species found on nearshore rocky bottoms at depths of 10–100 m. They are mainly residing in the oceans around Korean peninsula, Japan and China which harbors shallow rocky shores along the coastal line. *S. schlegeli* exhibits the fastest growth among rockfishes and has been cherished recently, due to its good characteristics such as tolerance to low water temperature, fast growth with higher survival rate. Production of black rockfish is second only to that of olive flounder (*Paralichthys olivaceus*) production in marine fish aquaculture in the Republic of Korea. The mass production of black rockfish in Korea was established in the early 1990s; since then, black rockfish, which stagnates on the southern coast, has become a representative aqua crop species in Korea. Since 2001, production has been increased and in 2013, 23,757 tons were produced while the production of flounder was 36,944 tons (Hwang et al., 2014). By today, these two species comprise 80% of the fish culture output of Korea. However, the production losses also encountered with this aqua-crop mainly due to the prevalence of infectious diseases, affirming that pathogen control is a crucial factor to obtain good production of this fish in both quality and quantity wise.
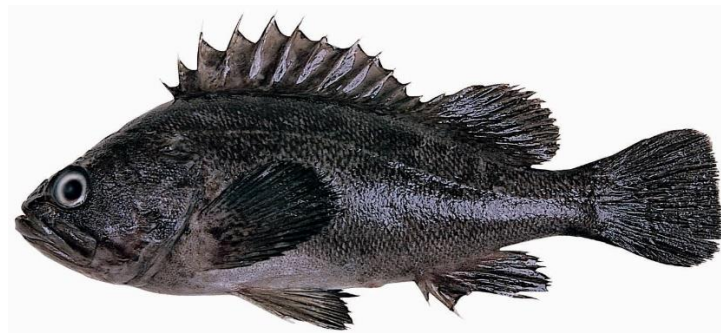
Fig. 1. Black rockfish (*Sebastes schlegeli*)

Glutathione (GSH), L-Glutamyl-L-cysteinyl-glycine (Fig. 2), is a soluble antioxidant, recognized as the most important non-protein thiol present in all living organisms. It consists of three amino acids (Glu-Cys-Gly), and it is the cysteine thiol group of the active site that is responsible for its biochemical properties. GSH is the most abundant non-protein molecule which acts as a reductant and free radical scavenger providing protection through non-enzymatic mechanisms on the other hand accompanied with many other roles in cellular level such as, modulation of cell proliferation, apoptosis, fibrogenesis and most importantly immune functions (Balendiran et al., 2004; Lu, 2013).
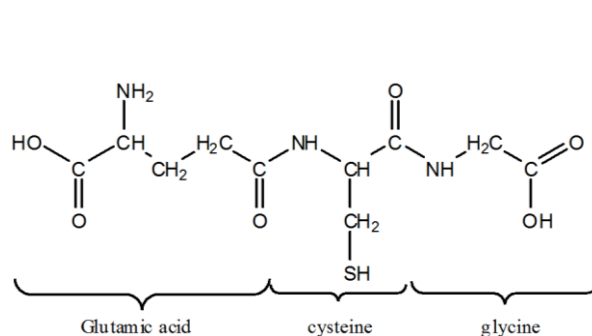
Fig. 2. Chemical structure of glutathione (GSH)

Xenobiotic metabolism can be divided in to three different phases such as phase I, phase II and phase III. Phase I enzymes oxidize, hydrolyze or reduce the state of the xenobiotic and add a reactive group converting the compound utilizable by the phase II enzymes which conjugate the substrate converting it more water soluble and capable to excrete with the phase III enzymes. The conjugated products which have been increased their solubility are readily expellable from the cell.

Glutatione S-transferases (GSTs, EC 2.5.1.18) are coming under the phase II enzymes which are an important multifunctional family of proteins with fundamental roles in the cellular detoxification of a wide range of exogenous and endogenous compounds (Frova, 2006). GSTs catalyze the reduced glutathione (GSH) to form thiolate (GS^-), the anion and form a complex with GST which nucleophilically attack the close by electrophilic xenobiotics. GSTs undergo

different transcriptional and posttranscriptional modification and gain the ability to modulate resistance to specific xenobiotics (Hayes and Pulford, 1995). In addition, GSTs are to be functioned as peroxidases, isomerases and thiol transferases or non-catalytically function by binding of non-substrate ligands and modulating signaling processes (Frova, 2006). Due to their role in detoxification, GSTs have been identified as an important category in development of drugs, antibiotics, insecticides and pesticides.

GSTs can be found among almost all the kingdoms and their existence in the kingdoms of Eubacteria, Protista, Fungi, Plantae and Animalia has been already proven (Hayes and Pulford, 1995). GSTs are divided into three distinct supergene families; according to their chemistry, immunological properties, kinetics and structural properties.

1. The soluble or cytosolic GSTs

2. MAPEG (membrane- associated proteins involved in eicosanoid and glutathione metabolism) / microsomal GSTs

3. The plasmid-encoded bacterial fosfomycin-resistance GSTs

The number of GST subfamilies may be larger than expected while there are many related families have been identified with the thioredoxin fold i.e. glutaredoxins (GRX), chloride intracellular channels (CLIC), dehydroascorbatereductases (DHAR), selenocysteine glutathione peroxidases (SecGPX), bacterial DsbA and eukaryotic protein elongation factors (eEF1Bg) (Frova, 2006). Cytosolic GSTs are further subdivided into several classes according to their structural, functional and locational variances as alpha, beta, delta, epsilon, zeta, theta, mu, nu, pi, sigma, tau, phi, rho, kappa, omega, elongation factor 1 gamma, dehydroascorbate reductase (DHAR) and tetrachlorohydroquinone dehalogenase. Microsomal GST and leukotriene C_4 synthase are categorized under MAPEG group (Calvin et al., 1975; Frova, 2006).

Cytosolic GSTs are active as either homodimer form or heterodimer form, each encoded by independent genes. Hetero-dimerization occurs in between same class subunits where

different class subunits may difficult to form a dimer due to their interfacial residue incompatibility (Frova, 2006). However, lambda class GST and DHAR was found to be active in monomeric form which lacks in GSH- dependent conjugating and peroxidase activities with standard substrates (Dixon et al., 2002). They are categorized as GSTs on the basis of sequence and structure similarity and in narrow sense, they share other GST catalytic properties such as thiol transferase activity (Frova, 2006).

A cytosolic GST, GST omega (GSTω) distinctly differs from the other GSTs with the presence of N-terminal extension rich in Proline (19-20 residues) and possessing a unique cysteine residue at the active sites that can form a disulfide bond with GSH (Calvin et al., 1975; Sheehan et al., 2001). The presence of cysteine promotes mixed disulphide formation with glutathione other than thiolate anion formation. As the major function of GSTω, it acts as a GSH dependent S-thiole transferase by removing the S⁻thiol from some proteins which bound to GSH via cysteine under the oxidative stress (Board et al., 1995). Other than the thiol transferase activity, GSTω shows dehydroascorbate reductase and monomethyl arsenate reductase activities (Schmuck et al., 2005). However, GSH conjugating activity by GSTω is minute (Board et al., 1995). Up to date, teleost GSTω has been characterized in *Oncorhynchus kisutch* (Espinoza et al., 2013) and *Danio rerio* (Glisic et al., 2015).

GST rho (GSTρ), a cytosolic GST, has been identified as a fish specific GST in numerous studies (Konishi et al., 2005; Liang et al., 2007) but, recently it has been reported to be present in mollusks as well (Park et al., 2013). As a group, GSTρ shares more than 80% homology among aquatic animals (Konishi et al., 2005). The first GSTρ has been identified and characterized from *Pragus major* (Konishi et al., 2005) and thereafter, GSTρ has been characterized in *Oreochromis niloticus* (Yu et al., 2014), *O. kisutch* (Espinoza et al., 2013) and *D. rerio* (Glisic et al., 2015). The function of GSTρ has not been defined yet but, suggested

4

that, GSTρ may protect fish tissues against oxidative damage associated with changes in membrane fluidity (Espinoza et al., 2013).

Theta class GST (GSTθ), another cytosolic GST which is different from the other related GSTs such as Alpha, Mu and Pi class not only in structure but also in function (Board et al., 1995). GSTθ demonstrated minute or non-detectable activity towards the model substrate of the GSTs; 1-chloro-2,4-dinitrobenzene (CDNB) and in the place of N-terminal tyrosine, GSTθ possesses a serine residue (Blocki et al., 1993; Board et al., 1995). GSTθ has been identified and characterized from teleost species au courant such as *Rivulus marmoratus* (Lee et al., 2006) and *D. rerio* (Glisic et al., 2015).

In the present study, three paralogs of GST family; GSTω, GSTρ, and GSTθ from black rockfish (*Sebastes schlegeli*) were identified using a previously established cDNA database and with the help of NCBI-BLAST tool and molecularly characterized. In order to investigate their biochemical characteristics and antioxidant dimensions to protect the fish from the xenobiotic stress, the three paralogs were independently cloned and subjected to various assays. Furthermore, to investigate the response upon bacterial and viral stimuli, black rockfish were undergone challenge experiments with live *Streptococcus iniae* bacteria and polyinosinic:polycytidylic acid (poly I:C). The temporal transcriptional modulation of these three genes upon challenge experiments was investigated using quantitative real time PCR (qPCR).

2. MATERIALS AND METHODS

2.1 Experimental fish, husbandry and tissue collection

Healthy black rock fish weighing 200 g which were pre-acclimatized to the laboratory conditions were obtained from Marine Science Institute of Jeju National University, Jeju self-governing province, Republic of Korea. The fish were maintained in 400 L laboratory aquarium tanks filled with aerated water at 22 ± 1 °C. Five healthy unchallenged fish were used to collect blood samples (~1 mL / fish) from the caudal fin into sterile syringes coated with 0.2% heparin sodium salt (USB, USA). The harvested blood cells were immediately centrifuged at $3000 \times g$ in 4 °C for 10 minutes. Nine tissues namely; head kidney, spleen, liver, gill, intestine, kidney, heart, male gonad, female gonads were incised from five healthy fish and all the harvested tissues and blood were snap-frozen and stored in -80 °C until further use.

2.2 Chemicals and reagents

Glutathione reduced (GSH), Dehydro ascorbate (DHA), 1-chloro-2,4-dinitrobenzene (CDNB), 1, 2-dichloro-4-nitrobenzene (DCNB), ethacrynic acid (ECA), 4- nitrobenzyl chloride (4-NBC), 4-nitrophenethyl bromide (4-NPB), hematin porcine, and Bradford reagent were purchased from Sigma-Aldrich, Republic of Korea. Cibacron blue (CB) was purchased from Polyscience Inc., USA. Isopropyl-β-D-thiogalactopyranoside (IPTG) was obtained from Promega, USA. Protein markers were obtained from Enzynomics™, Republic of Korea. Commercially available poly I:C was attained from Sigma, USA. All the other chemicals were of analytical grade.

제주대학교 중앙도서관
JEJU NATIONAL UNIVERSITY LIBRARY

2.3   Preparation of Black rockfish cDNA sequence database

By using Roche 454 genome sequencer FLX (GS-FLX^{TM}) (Droege and Hill, 2008) system, the black rock fish cDNA library was prepared. Briefly, the total RNA was extracted from blood, liver, kidney, gill and spleen tissues of three different fish. The extracted RNA was then cleaned by RNeasy Mini kit (Qiagen, USA) and assessed for quality and quantified using an Agilent 2100 Bioanalyzer (Agilent Technologies, Canada), which detects an RNA integration score (RIN) of 7.1. For GS FLX 454 shotgun library preparation, the RNA was fragmented into average size of 1,147 bp using the Titanium system (Roche 454 Life Science, USA). Sequencing was finally run on half a picotiter plate on a Roche 454 GS FLX DNA platform at Macrogen, Republic of Korea. The raw 454 reads were trimmed to remove adaptor and low-quality sequences, and *de novo* assembled into contigs using GS Assembler (Roche 454 Life Science, USA) with the default parameters.

2.4   Identification and sequence analysis of three GSTs from the black rockfish

Full length cDNA sequences of black rockfish GSTω, GSTρ, and GSTθ (*RfGSTω*, *RfGSTρ*, and *RfGSTθ*, respectively) were identified from this database using the Basic Local Alignment Tool (BLAST) in the National Center for Biotechnology Information (NCBI) web based query system (http://www.ncbi.nlm.nih.gov/BLAST) using the default algorithm parameters. The open reading frame (ORF) and amino acid (aa) sequence of the putative proteins were analyzed using DNAssist software (version 2.2). Matrix Global Alignment Tool (MatGAT) v2.01 was used to analyze the identities and similarities of the relevant proteins with their orthologs.   Multiple sequence alignment was carried out with the help of ClustalW2 (http://www.ebi.ac.uk/Tools/clustalw2/index.html)   and   color   align   conservation (http://www.bioinformatics.org/sms2/color_align_cons.html) web based software. ExPASy

prosite (http://prosite.expasy.org) was used to find the conserved domains while SignalP 4.1 server (http://www.cbs.dtu.dk/services/SignalP) was used to find the signal peptide sequence. MEGA 6 software (Tamura et al., 2013) (http://www.megasoftware.net) was used to analyze the evolutionary distances among GST orthologs as well as the GST paralogs by constructing a gene tree using the neighbor-joining (NJ) method with the bootstrap support of 1000 replicates.

The three dimensional models of each paralog were fabricated using the I-TASSER server and subjected to the molecular docking with GSH (DrugBank ID: DB00143) as the ligand using Hex 8.0 (Ritchie et al., 2008). The Ramachandran plot (Ramachandran et al., 1963) was used to validate the proposed model. The successfully docked models were analyzed to ascertain their protein-ligand interactions using LigPlot+ v.1.4.5 (Wallace et al., 1995).

2.5   Immune challenge experiments

To determine the transcriptional responses against the stimulation of *S. iniae* as a live bacterial pathogen (1×10^5 CFU/μL) and poly I:C (1.5 μg/μL) as a double stranded RNA viral mimic, immune challenges were employed. *S. iniae* was obtained from Department of aquatic medicine, Chonnam National University, Republic of Korea. Respective stimuli were used to inject the healthy fish after resuspending or dissolving in $1 \times$ phosphate buffered saline (PBS). Fish were intraperitoneally (i.p.) injected with each stimulant in a total volume of 200 μL. For the injection control, a group of fish injected with 200 μg PBS alone was used. Thereafter, blood and liver tissues from five injected fish were collected at 3, 6, 12, 24, 48, and 72 h post-injected time points, corresponding to each challenge as described in the section 2.1.

2.6 RNA isolation and first-strand cDNA synthesis

QIAzol® (Qiagen) reagent was used to extract total RNA from the tissue samples (both challenged and healthy fish) weighing ~ 40 mg each from five individual fish following the manufacturer's protocol. RNA quality was examined by 1.5% agarose gel electrophoresis and the concentration was determined at 260 nm in μDrop Plate (Thermo Scientific). The first-strand cDNA synthesis was carried out using the PrimeScript^{TM} II first-strand cDNA synthesis Kit (TaKaRa, Japan) following the manufacturer's protocol where 2.5 μg of RNA was used. The synthesized cDNA was diluted 40-fold in nuclease free water and stored at -80 °C for further use.

2.7 Cloning of three GST paralogs into the pMAL-c5X expression vector

To clone the coding region of each GST paralog into the expression vector pMAL-c5X (New England Biolabs, USA), primers were designed with NdeI and EcoRI restriction sites (Table 1). Using TaKaRa thermal cycler (Japan), the coding regions were amplified. For the PCR amplification, ExTaq^{TM} DNA polymerase (TaKaRa, Japan) was used. The amplified products were then digested with the respective restriction enzymes along with the pMAL-c5X vector simultaneously. The digested products were then ligated in a mixture of 10 μL containing MightyMix (TaKaRa, Japan) at 16 °C for 30 minutes and incubated overnight at 4 °C. The resulted product was then transformed into *Escherichia coli* DH5α cells and confirmed the ligation was ensued via gel electrophoresis with 1% agarose and sequencing.

Table 1. The primers used in this study

Primer Name	Application	Sequence of Primer (5'-3')
RfGSTω_F		(GA)$_3$catatgATGTCTACTGAGAAGTGTTTCGCCAAAGG - NdeI
RfGSTω_R		(GA)$_3$gaattcCTACAGGCCATAGTCGTAGTTGGGTTTC - EcoRI
RfGSTρ_F		(GA)$_3$catatgATGGCCCAGGACATGACTCTGC - NdeI
RfGSTρ_R	ORF amplification	(GA)$_3$gaattcTCAGATGTCTTTGAGTGTGTCTTGTCCTTTG - EcoRI
RfGSTθ_F		(GA)$_3$catatgATGGAGCTCTATCTGGACCTGTTCTCT - NdeI
RfGSTθ_R		(GA)$_3$gaattcTCAGCTGAACATCTTTTGAAGCTTTAGTTTGAACT - EcoRI
RfGSTω_qF		TTCGCCCACAGGACCAGATTAGT
RfGSTω_qR		ACCAGCAGGTGTCTCCAGAGTT
RfGSTρ_qF	qPCR amplification	ACAAGGAAGCTCTGATCACCGAAGTC
RfGSTρ_qR		CACATCTGCCAGAGAGAAGGATGGT
RfGSTθ_qF		AGGCTCTGAATCAGTCGCTCACAA
RfGSTθ_qR		TATAGCCACCAGATCAGCCAGAGAGA
RfEF1α_qF	qPCR internal reference	AACCTGACCACTGAGGTGAAGTCTG
RfEF1α_qR		TCCTTGACGGACACGTTCTTGATGTT

2.8   Expression and purification of recombinant proteins

The sequence confirmed ligated products of pMAL-c5X/RfGST were transformed into competent *E. coli* ER2523 (New England Biolabs, USA) for protein expression. A single colony bearing positive vector was incubated at 37 °C overnight in LB broth containing 100 µgmL^{-1} ampicillin. Subsequently the fraction of culture was transferred (1:100) into LB rich medium supplemented with glucose (2 gL^{-1}) and ampicillin (100 µgmL^{-1}). IPTG was added (0.5 mM final concentration) into the culture which reached ~0.5 optical density at 600 nm and incubated for approximately 10 hours at 20 °C facilitating the induction of protein expression.

The cells were harvested under 3500 rpm for 30 min at 4 °C and the harvested cells were re-suspended in column buffer (Tris–HCl, pH 7.4, 200 mM NaCl, 0.5 M EDTA) and, stored at -20 °C overnight. The thawed cells were then sonicated on ice prior centrifugation at 13000 rpm for 30 min at 4 °C. The supernatant was allowed to flow according to gravity through amylose resin and the recombinant protein bound resin was washed with 12 volumes of column buffer. Then the recombinant proteins were collected with elution buffer (column buffer + 10 mM maltose) as 0.5 mL fractions. Finally the concentration of collected fusion proteins were measured using the Bradford method (Bradford, 1976) while the purity was analyzed using the SDS polyacrylamide gel electrophoresis (SDS-PAGE).

2.9　Functional characterization of recombinant GST paralogs

2.9.1　GST enzyme assay

The specific activity of recombinant proteins was measured with various substrates including CDNB, DCNB, 4-NPB, 4-NBC, ECA and DHA. A reaction mixture was prepared with 1 mM reduced GSH, appropriate amounts of respective protein (rRfGSTs) and phosphate buffer. The absorbance of the reaction was measured at corresponding wave length as soon as the addition of 1 mM substrate to the mixture and after 5 minutes from the addition of substrate. The final volume of whole reaction mixture was kept as 200 µL and the temperature was maintained at 25 °C. All the assays were performed in triplicates. The substrate specific parameters are listed in Table 2.

Table 2. Substrate specific parameters

Substrate	Substrate (mM)	GSH (mM)	pH	Temperature (°C)	λmax (nm)	Molecular extinction coefficient (ϵ) (mM^{-1} cm^{-1})
CDNB	1.0	1.0	6.5	25	340	9.6
DHA	1.0	1.0	6.85	25	265	14.7
DCNB	1.0	1.0	7.5	25	345	8.5
4-NPB	1.0	1.0	6.5	25	310	1.2
4-NBC	1.0	1.0	6.5	25	310	1.9
ECA	1.0	1.0	6.5	25	270	5.0

2.9.2 Michaelis–Menten kinetics

The activity of recombinant proteins was measured as described in 2.8.1 with the different concentrations of the respective substrate (0.25–4.0 mM) while the GSH concentration was kept constant at 1 mM. DHA was used in the instance of RfGSTω and, CDNB was used in the instances of GSTρ, and GSTθ as the substrate. The Michaelis constant (K_m) and the maximum reaction velocity (V_{max}) values of the respective substrate were analyzed using the Lineweaver–Burk plot (Lineweaver and Burk, 1934). The same assay was conducted with various concentrations of GSH (0.25–4.0 mM) to ascertain the K_m and V_{max} of GSH where the substrate concentration was kept constant at 1 mM.

2.9.3 The effect of pH, the effect of temperature and the responses upon inhibitors

The effect of pH to the activity of recombinant proteins with CDNB (rRfGSTρ and rRfGSTθ) and DHA (rRfGSTω) was determined using a buffer series ranged from 3 pH ~ 10 pH (Acetic-acetate buffer (10 mM, pH 3 – 5), sodium phosphate buffer (10 mM, pH 6 – 7), Tris–HCl buffer (10 mM, pH 8 – 9), and Glycine-NaOH buffer (10 mM, pH 10)). Here, all the conditions other than the pH buffer retained as described in 2.9.1. The effect of the temperature upon activity of each protein towards the corresponding substrate was determined using water baths ranged from 10 °C to 60 °C. To determine the behavior of the three proteins upon inhibitors, two commercially available GST inhibitors CB (0.0001–100 μM) and hematin (0.0001–100 μM) were used as previously reported (Tahir et al., 1985).

2.10   Disk diffusion assay

Disk diffusion assay was performed in order to compare the survival efficacy of untransformed *E. coli* (u-EC), transformed *E. coli* with RfGSTs/MBP fusion vectors (ω-EC, ρ-EC and θ-EC, respectively), and transformed *E. coli* with only pMAL c5x vector (v-EC) upon oxidative stress and heavy metals as described earlier (Lee et al., 2007). Briefly, all bacteria were cultured in 0.5 mM IPTG added LB media for 4 h at 25 °C. Each bacterium was individually and equally spread over LB agar plates. Four Whatman filter-paper disks (3 mm diameter) were placed onto the agar plate in equal distance and each disk was treated with 5 μL of H_2O_2, 1M $CdCl_2$, 1M $CuSO_4$ and 1M $ZnCl_2$ respectively. The plates were incubated at 37 °C overnight and the diameter of the zone of clearance was recorded.

2.11   Transcriptional analysis by qPCR and statistical analysis

To determine the basal transcript levels of each GST paralog in collected tissues of healthy fish and to analyze their transcriptional modulation in injected fish, qPCR assay was performed using gene specific primers and synthesized cDNA as templates. Each primer pair were designed assuring the amplicon size ~150 bp, GC content ~ 50% and melting temperature ~ 60 °C (Table 1). Assay was performed using the Dice^{TM} Real time system thermal cycler (TP800; TaKaRa, Japan) in a 10 μL reaction volume containing 3 μL of diluted cDNA from each tissue, 5 μL of 2x TaKaRa ExTaq^{TM} SYBR premix, 0.8 μL of each primer pair and 1.2 μL of ddH_2O. The thermal cycling conditions were kept as one cycle of 95 °C for 10 s, followed by 45 cycles of 95 °C for 5 s, 58 °C for 20 s, 72 °C for 20 s and a final single cycle of 95 °C for 15 s, 60 °C for 30 s and 95 °C for 15 s. Triplicates of each assay were analyzed with automatic baseline parameters of the Dice™ Real Time System software (version 2.00). The Livak and Schmittgen's $2^{-\Delta\Delta CT}$ method (Livak and Schmittgen, 2001) was employed to quantify the

14

transcriptional modulation. Using the same PCR cycling conditions, elongation factor -1-alpha of black rock fish (RfEF1A; KF430623) was quantified in order to normalize the GST transcripts in each qPCR assay.   Each challenged sample was normalized to the corresponding PBS-injected control at each time point while the un-injected control at the 0 h time point was used as the basal level reference. Final expressional data were used as mean relative mRNA expression ± standard deviation (SD).

2.12   Statistical analysis

To determine statistical significance between experimental data and controls, data were subjected to statistical analysis by one-way analysis of variance (ANOVA) and the mean comparison was carried out by Duncan's multiple range test using SPSS 16.0 statistical software where the significance level was defined as $p < 0.05$.

3. RESULTS

3.1   Sequence characterization of *RfGSTω*, *RfGSTρ*, and *RfGSTθ*

The full length cDNA sequence of *RfGSTω* (GenBank accession No: KT322171) consisted with 66 bp 5′ untranslated region (UTR) and 395 bp 3′ UTR, where the open reading frame (ORF) of 717 bp was lied in between (Fig. 3A). Polyadenylation signal was found to be appeared as ^{957}AATAAA^{962} at the 3′ UTR. The putative protein encoded by the ORF was 239 amino acids in length and 28 kD in molecular weight. The predicted isoelectric point was 7.4.

Fig. 3A. Nucleotide and deduced amino acid sequence of RfGSTω. The start (ATG) and stop codon (TAG) are boxed. Unique proline rich N - terminal extension is shaded in dark gray. The N- terminal domain and C - terminal domain are shaded in light gray and black, respectively. The poly A signal (AATAAA) is in boldface.

RfGSTρ full length cDNA sequence (GenBank accession No: KT322170) consisted with 36 bp 5′ UTR, 395 bp 3′ UTR and 678 bp ORF (Fig. 3B). Polyadenylation signal was appeared as [909]AATAAA[914] at the 3′ UTR. The putative protein was 226 amino acids in length. The molecular weight of the putative protein was 26 kD and the predicted isoelectric point was 5.8.

```
                                        CTCACT CCACTCAAGCCTGTC AGATCTACAACCACC    -36
ATGGCCCAGGACATG ACTCTGCTGTGGGGC TCCGGCTCTCCTCCC TGCTGGAGGGTCATG ATCGCTCTGGAGGAG AAGAACCTGCAGGGC     90
 M  A  Q  D  M   T  L  L  W  G    S  G  S  P  P   C  W  R  V  M   I  A  L  E  E   K  N  L  Q  G     30
TACAACCAGAAACTG CTCTCCTTTGAGAAA ATGGAGCACAAGTCC CAAGAAGTGCTAGAT ATAAATGCCAGGGGA CAGCTTCCCTCTTTC    180
 Y  N  Q  K  L   L  S  F  E  K   M  E  H  K  S   Q  E  V  L  D   I  N  A  R  G   Q  L  P  S  F     60
AAGCACGGAGACGTC ATTGTGAATGAATCC TATGCAGCTTGTTTT TACCTGGAGAGTCAG TTTAAGTCTGAGGGA ACCAAACTGATCCCA    270
 K  H  G  D  V   I  V  N  E  S   Y  A  A  C  F   Y  L  E  S  Q   F  K  S  E  G   T  K  L  I  P     90
GACAGCCCGGCAGAA CAAGCACTAATGTAC CAACGCATGTTTGAG GGTCTCTCATTCTAC GAAAAACTCAATACA GTTACCTACTATGAC    360
 D  S  P  A  E   Q  A  L  M  Y   Q  R  M  F  E   G  L  S  F  Y   E  K  L  N  T   V  T  Y  Y  D    120
TGGTTTGTCCCTGAA GGAGAGAGGCATGAC TCAGCACTAAAGAGA AACAAGGAAGCTCTG ATCACCGAAGTCAAG CTCTGGGAGGGTTAC    450
 W  F  V  P  E   G  E  R  H  D   S  A  L  K  R   N  K  E  A  L   I  T  E  V  K   L  W  E  G  Y    150
CTGCAGAAGCTGGGC TCGGGTTCTCACCTG GCGGGACCATCCTTC TCTCTGGCAGATGTG ACCGTTTTTCCAACT GTTGCTACTCTTTC     540
 L  Q  K  L  G   S  G  S  H  L   A  G  P  S  F   S  L  A  D  V   T  V  F  P  T   V  A  T  L  F    180
AGATTTGGGTTGTCT GCAGAGCGTTACCCT AAACTGGGAGAGTAT TACGCTCTGCTGAAG GAGCGGCCCAGCGTC AAAGCCAGCTGGCCT    630
 R  F  G  L  S   A  E  R  Y  P   K  L  G  E  Y   Y  A  L  L  K   E  R  P  S  V   K  A  S  W  P    210
CCTCACTGGCTAGAG AACCCCAAAGGACAA GACACACTCAAAGAC ATCTGAGATCCACAC ACACTTTTAAAGTCA CGTCTGCCCATAATG    720
 P  H  W  L  E   N  P  K  G  Q   D  T  L  K  D   I  *                                             240
TTTTGGTTTCTATAA AAATGCTTTTGTTCA ATAGGGAAAAAAGTG TTGAGTTCACAAGTA TGTTCTAAATATATT AGTGTTACAAGGGCA    810
GAATGTGCTTGTTTT GTTTTTTGTCAAACT AGCTTTTATATTTAG TTTAAAGGTTTTTGT CCATCATATTTCTGT CAAATGTTTGATAAA    900
AATCTGTTAATAAAC                                                                                   915
```

Fig. 3B. Nucleotide and deduced amino acid sequence of RfGSTρ. The start (ATG) and stop codon (TAG) are boxed. The N- terminal domain and C - terminal domain are shaded in light gray and black, respectively. The poly A signal (AATAAA) is in boldface.

The full length cDNA sequence of *RfGSTθ* (GenBank accession No: KT322172) consisted of an ORF 720 bp which was lied in between 56 bp 5′ UTR and 169 bp 3′ UTR (Fig. 3C). The polyadenylation signal was [893]ATTAAA[898] and found at the 3′ UTR. The putative protein encoded by the ORF was 240 amino acids while the molecular weight and the theoretical isoelectric point were 28 kD and 8.4, respectively.

```
                                 GAAGACACAGA AAGGAACGCTTTGGA AAGGAACACTCTCAC ACTCACACTGACATG      -56
ATGGAGCTCTATCTG GACCTGTTCTCTCAG CCCTGCCGCTCCGTC TTCCTGTTTGCCAAA ACTGTCGGGATTCCC TTTGACTTGAAGCTG       90
 M  E  L  Y  L   D  L  F  S  Q   P  C  R  S  V   F  L  F  A  K   T  V  G  I  P   F  D  L  K  L        30
GTGGAACTTACTAAA GGGCACCAGTATGAC GAGGACTTTGGAAAA GTCAACGTCATGAGG CAGGTTCCTGTCTTG AAGGATGGAAGCTTC      180
 V  E  L  T  K   G  H  Q  Y  D   E  D  F  G  K   V  N  V  M  R   Q  V  P  V  L   K  D  G  S  F        60
GTTCTGACGGAGAGC ACTGCGATCCTGAGG TACCTGGTGCAGAAG CATTCGGTGGCAGAT CACTGGTATCCAGCT GAGCTGCAGCAGCGA      270
 V  L  T  E  S   T  A  I  L  R   Y  L  V  Q  K   H  S  V  A  D   H  W  Y  P  A   E  L  Q  Q  R        90
GCTCGTGTTAACGAA TATCTGTCCTGGCAG CACACGAACCTCAGA GCCCACGGGTCGAAG GTCTTCCTGTTCAGG GCTCTGTATCCTGTC      360
 A  R  V  N  E   Y  L  S  W  Q   H  T  N  L  R   A  H  G  S  K   V  F  L  F  R   A  L  Y  P  V       120
GTCATGGGAACCGAG GTCCCGAAGGAGAAG ATGGACGCGGCTCTC GAGGCTCTGAATCAG TCGCTCACAATGGTG GAGGAGAAATTCCTG      450
 V  M  G  T  E   V  P  K  E  K   M  D  A  A  L   E  A  L  N  Q   S  L  T  M  V   E  E  K  F  L       150
CAGAACAAACCGTTC ATCATCGGCGACAAA ATCTCTCTGGCTGAT CTGGTGGCTATAGTT GAGATCATGCAGCCT TTTGGAACCCGCCTG      540
 Q  N  K  P  F   I  I  G  D  K   I  S  L  A  D   L  V  A  I  V   E  I  M  Q  P   F  G  T  R  L       180
GACGTGTATGAAGGG CGGCCGAAGCTGATC GCCTGGAGGGATCGA GTGAAGAAGGTGATC GGTGAAAAGTTGTTT GACGAAGCTCACGAG      630
 D  V  Y  E  G   R  P  K  L  I   A  W  R  D  R   V  K  K  V  I   G  E  K  L  F   D  E  A  H  E       210
GTGATCATGAAGGCG CCCAATCTGGCGGAG GAGATGAAGAACAAT ACGGATCTGGAGAAG TTCAAACTAAAGCTT CAAAAGATGTTCAGC      720
 V  I  M  K  A   P  N  L  A  E   E  M  K  N  N   T  D  L  E  K   F  K  L  K  L   Q  K  M  F  S       240
TGAGTACAAACAGTT TATACGACTGTGGAT GGTGTCCGAAAATTA TGTTAATTTGAATCT AATGTGCCACGTTTT ATTATCAGCATCCTT      810
 *
TTTTAATTAGCCTCC TTTTTTATCATTATC CTGTGCAGGTTTGTC ATGAAGTACTGAGAA ATCATTTACCCAGCT TCCACGTATTAAACT      900
GTTAAAGTGTGCACG TTGTGTAAATATTTG TGTGAATGTAAACAA ATATGTTCATTTGAT TCAGATAGGCAAGGC AAGGCAAGACAAGGC      990
AGCTTGATAGATACC TACAGAAACAAACAG TATTTGGTCTGCCAA CAAAGAAAACACACT TAATTTTCATGCTAT AAATTCTGAAGGAAA     1080
TCTAGAAACTGTTCA ACATTTCAGCTGGAA ATATTCACCATACCA TCACCAATATTCACC AACTCATTGTGTATT AAAGTGTTTTCCTCT     1170
TGAACTGTTATGAAT GAATGCACGTGCACT ATCCCCACACCCCAA ATATTAAAGTGAT                                       1228
```

Fig. 3C. Nucleotide and deduced amino acid sequence of RfGSTθ. The start (ATG) and stop codon (TAG) are boxed. The N- terminal domain and C - terminal domain are shaded in light gray and black, respectively. The poly A signal (AATAAA) is in boldface.

3.2   Pairwise and multiple sequence alignment analysis

Pair-wise sequence analysis result revealed that RfGSTω shared higher identity and similarity with *Oplegnathus fasciatus* (ADY80021) compared to other orthologs with 95.8% and 92.5% respectively. However, all the orthologs considered in this study showed identities over 70% and similarities over 50% (Table 3).

In pair-wise sequence analysis of RfGSTρ with its orthologs, it shared higher identity and similarity with *Oreochromis niloticus* (ACT22666) compared to other orthologs (85.7% and 93.0% respectively). Fish counterparts shared identities over 70% and similarities over 80% while mollusks shared less than 50% identities and less than 70% similarities (Table 4).

RfGSTθ shared its highest identity (74.4%) and similarity (89.7%) with *Anoplopoma fimbria* GSTθ (ACQ58539) counterpart. Here, fish GSTθ counterparts showed more than 50% identities and similarities with RfGSTθ (Table 5).

Table 3. Percentage of interspecies amino acid sequence identity and similarity for RfGSTω

Organism	Species	Accession No.	I (%)	S (%)
Rock bream	*Oplegnathus fasciatus*	ADY80021	95.8	92.5
Sablefish	*Anoplopoma fimbria*	ACQ58017	91.2	86.6
Atlantic salmon	*Salmo salar*	NP_001134944	90.8	82.0
Mefugu	*Takifugu obscurus*	ABV24048	91.6	82.4
Coho salmon	*Oncorhynchus kisutch*	AGB56854	90.4	81.6
Zebrafish	*Danio rerio*	NP_001002621	87.1	75.8
Mangrove rivulus	*Kryptolebias marmoratus*	AEM65182	89.5	75.7
Northern pike	*Esox lucius*	ACO13714	85.4	70.3
African clawed frog	*Xenopus laevis*	NP_001099052	75.9	58.5
Chicken	*Gallus gallus*	NP_001264304	74.9	56.6
Cattle	*Bos taurus*	NP_001068682	74.3	56.6
Human	*Homo sapiens*	NP_004823	73.0	56.2
Chimpanzee	*Pan troglodytes*	NP_001233486	72.6	55.8

Table 4. Percentage of interspecies amino acid sequence identity and similarity for RfGSTρ

Organism	Species	Accession No.	I (%)	S (%)
Nile tilapia	*Oreochromis niloticus*	ACT22666	93.0	85.7
European plaice	*Pleuronectes platessa*	CAA64493	92.5	86.7
Red seabream	*Pagrus major*	BAD98442	86.7	73.5
Japanese flounder	*Paralichthys olivaceus*	ACE78286	83.2	75.7
Orange-spotted grouper	*Epinephelus coioides*	ACI01806	87.6	76.5
Atlantic salmon	*Salmo salar*	ACM08643	87.2	74.8
Coho salmon	*Oncorhynchus kisutch*	AGB56853	87.6	74.8
Lantern clam	*Laternula elliptica*	ACM44933	59.7	37.8
Disc abalone	*Haliotis discus discus*	EF103347	65.9	45.8
Venus clam	*Ruditapes philippinarum*	JN388954	55.3	39.7

Table 5. Percentage of interspecies amino acid sequence identity and similarity for RfGSTθ

Organism	Species	Accession No.	I (%)	S (%)
Sablefish	*Anoplopoma fimbria*	ACQ58539	74.4	89.7
Barred knifejaw	*Oplegnathus fasciatus*	ADY80024	72.8	88.5
Spotted snakehead	*Channa punctate*	ABY83769	69.1	86.8
Atlantic salmon	*Salmo salar*	ACI66470	66.0	81.6
Rainbow trout	*Oncorhynchus mykiss*	CDQ67100	65.2	81.1
Blue catfish	*Ictalurus furcatus*	ADO27893	59.9	79.3
Northern pike	*Esox lucius*	NP_001290604	57.0	76.3
Zebrafish	*Danio rerio*	NP_956878	57.6	74.4
Snakehead murrel	*Channa striata*	AFO70214	52.9	63.8
African clawed frog	*Xenopus laevis*	NP_001085203	53.1	71.5
House mouse	*Mus musculus*	CAA66666	50.4	69.7
Human 1	*Homo sapiens*	AAG02374	49.6	69.6
Human 2	*Homo sapiens*	AAB63956	41.2	66.8
Chicken	*Gallus gallus*	NP_990696	45.6	65.1
Cattle	*Bos taurus*	AAI11290	49.2	69.2

All three proteins were not possessed signal peptide according to the result assumed by the signalP 4.1 software. The ExPASy prosite database revealed that the RfGSTω consisted of a GST N-terminal domain (N^{20} - K^{99}) where GST binding site (G-site) lies within and, a C-terminal domain (S^{104} - V^{229}) where the substrate binding pocket (H-site) lies within (Fig. 4A). According to the results generated by the Pfam, the N-terminal domain of RfGSTρ was located at Q^3 - G^{85} while C-terminal domain was located at S^{92} - Q^{220} (Fig. 4B). In the instance of RfGSTθ, the N-terminal domain was lied at M^1 - D^{80} while C-terminal domain was at E^{86} - L^{228} (Fig. 4C).

The unique feature of GSTω protein, the Proline rich N-terminal extension could be identified at Met^1 - Val^{17} residues of RfGSTω (Fig. 4A). The active site could be identified as Cys^{30} of RfGSTω, Ser^{13} of RfGSTρ and Ser^9 of RfGSTθ (Fig. 4). The conserved *cis*-Proline residue of GST family could be identified in between α_2 and β_3 of RfGSTω (Pro^{71}), α_{2b} and β_3 of RfGSTρ (Pro^{58}) and, α_2 and β_3 of RfGSTθ (Pro^{53}) (Fig. 4). The number of α helices in the C-terminal domain of RfGSTω, RfGSTρ and RfGSTθ were 7, 7 and 10, respectively.
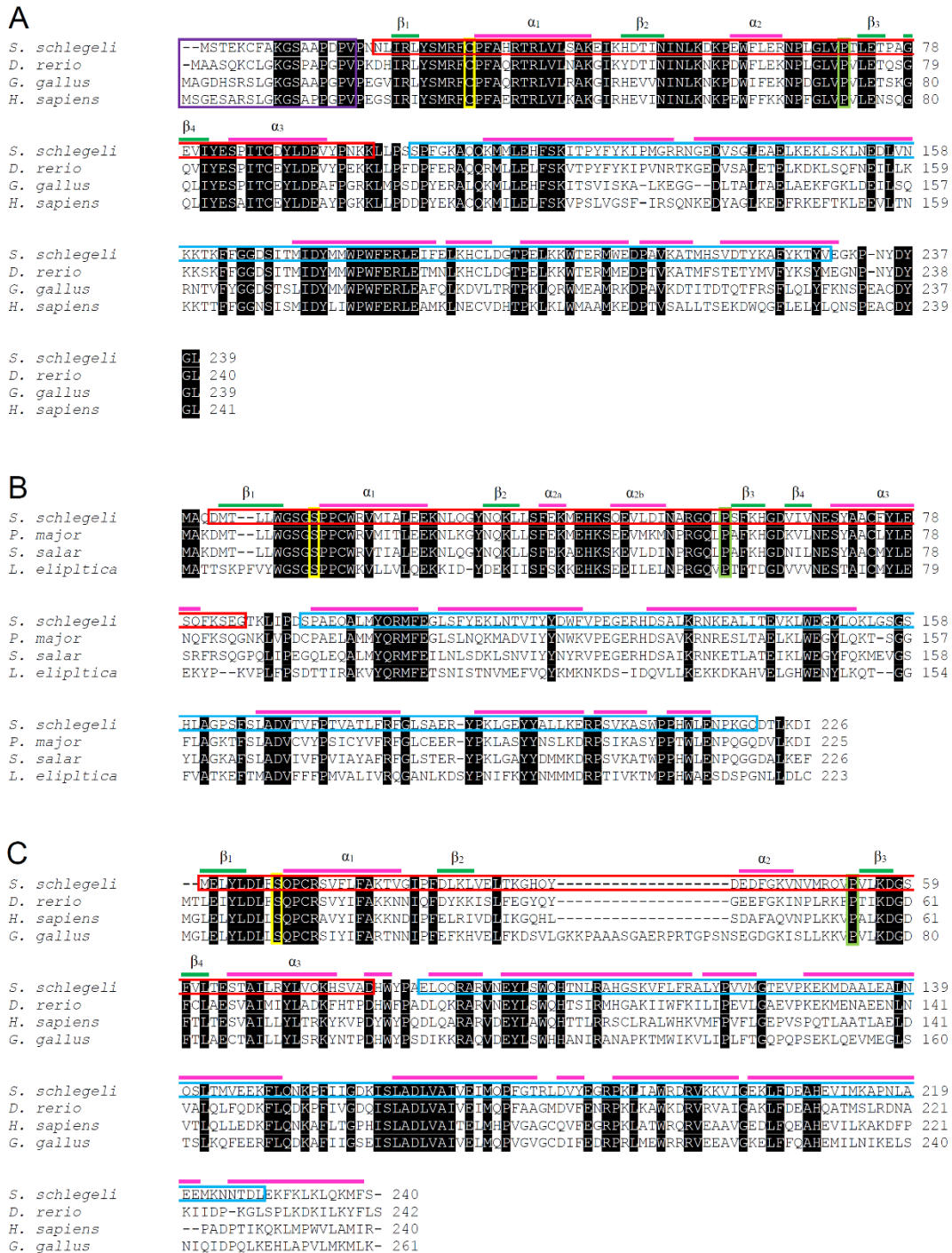
Fig. 4. Comparison of the derived amino acid sequences of RfGSTω (A), RfGSTρ (B), and RfGSTθ (C) with other organisms. Fully conserved residues are shaded in black. The N-terminal domain is boxed in red, while the C-terminal domain is boxed in blue. The β sheets are denoted in green lines and α helices in magenta lines on the sequence. The active site is boxed in yellow color and the conserved Proline residue is boxed in light green. The characteristic N-terminal extension of RfGSTω is boxed in purple.

3.3   Phylogenetic analysis of three GST paralogs

The gene family tree clearly and distinctly grouped into two main clusters where GSTκ and microsomal GST were grouped into one cluster, while all the cytosolic GSTs formed the other cluster. Three GST paralogs of the study were clearly parted into three different sister clusters in the cytosolic GST cluster (Fig 5). Furthermore, RfGSTω and RfGSTρ were clustered in one major cluster while RfGSTθ was clustered with other cytosolic GSTs.

The GSTω cluster has further subdivided into two sister clusters where mammals and non-mammals were parted from each other. In the non- mammals group where fish were lied, *Xenopus laevis*, an amphibian formed a basal cluster. RfGSTω was closely clustered with *Oplegnathus fasciatus* in the fish group. The other sister cluster has been further subdivided into two clades where aves and mammals were parted. In the GSTρ cluster, fish were grouped clearly into one sister cluster where RfGSTρ was clustered with *Pleuronectes platessa*. *Branchiostoma belcheri*, an amphioxus species was placed as an outlier of the fish group. Interestingly, *Haliotis discus discus*, a molluscan species was parted from its kind and placed as an outlier of the fish and amphioxus. GSTθ clade was further subdivided into two sister clades where fish and other species were parted from each other. In the fish group *D. rerio* formed a basal cluster. In the instance of RfGSTθ, it showed higher relationship to *P. platessa* GSTθ ortholog.

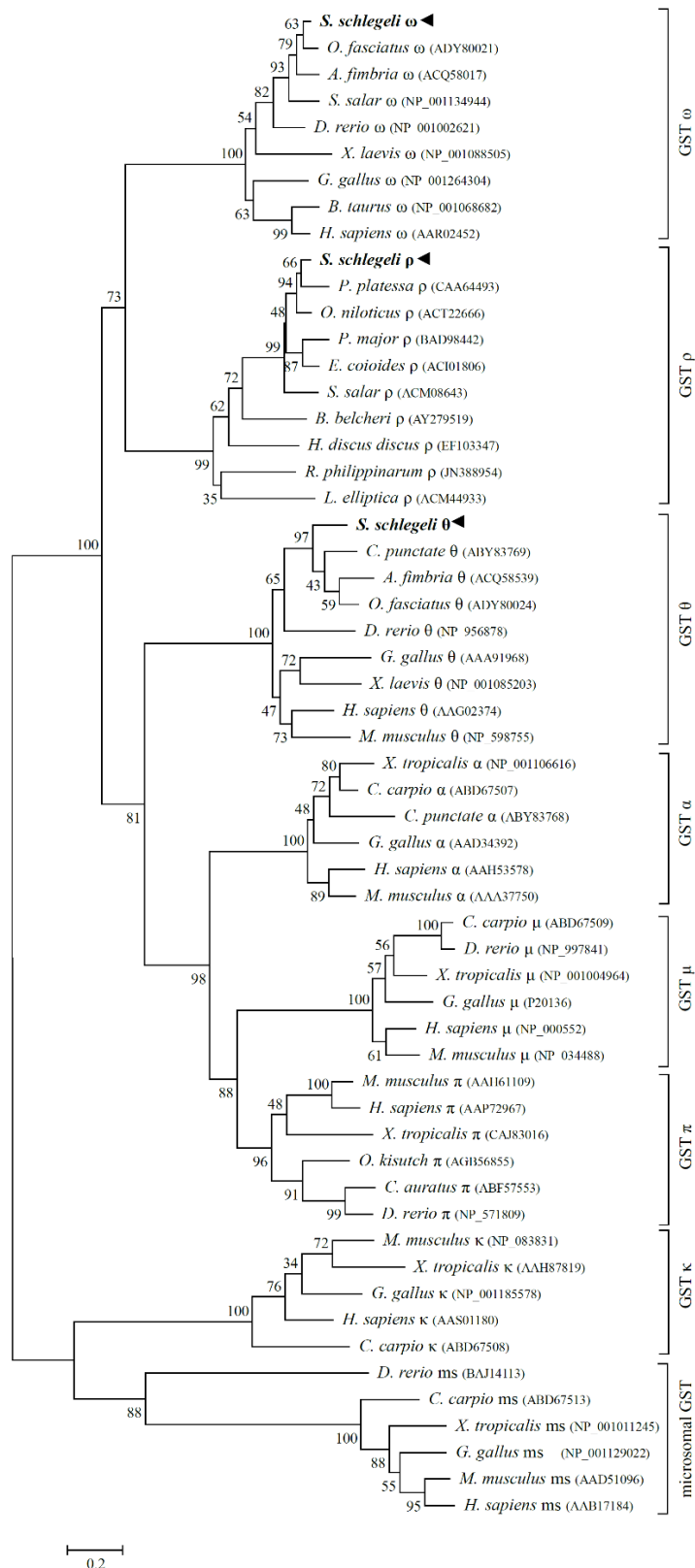**Fig. 5.** Consensus gene tree of GST counterparts formed using the neighbor-joining method. The bootstrap values are denoted next to each node of the gene tree. The accession numbers of each counterpart are along with the organism name.

3.4   Tertiary sequence characterization of three GST paralogs

The three dimensional model of RfGSTω was fabricated using the crystal structure of human GSTω (HsGSTω; PDB entry 1eem.1.A) which shared 55.5% identity and 46% similarity (Fig.6). GSH formed hydrogen bonds with Lys^{57}, Val^{70} and Ser^{84} of RfGSTω (Fig. 7A), while GSH formed the hydrogen bonds at Lys^{59}, Val^{72}, Glu^{85} and Ser^{86} in the instance of human GSTω (Fig. 7B). Additionally, a ligand bond could be identified between Sulfur atoms of GSH and Cys^{32} in HsGSTω.

Fig. 6. The modeled tertiary structure of RfGSTω. The strands, α helices and β sheets are represented in green lines, red coils and yellow arrows respectively.

A.

B.

Fig. 7. Schematic illustration of the molecular interactions between amino acid residues in RfGSTω (A) and Human GSTω (B)

The three dimensional model of RfGSTρ was generated using the crystal structure of *Laternula elliptica* GSTρ (LeGST; PDB entry 3qav.1.A) which shared 39.72% identity and 41% similarity (Fig. 8). In here, GSH formed hydrogen bonds with Leu[57] and Ser[70] of RfGSTρ while it formed ligand bonds with Ser[13] (Fig. 9A) while it formed hydrogen bonds with Ser[15], Lys[45], Gln[57], Val[58], Ser[71] and Glu[70] of LeGST (Fig. 9B).
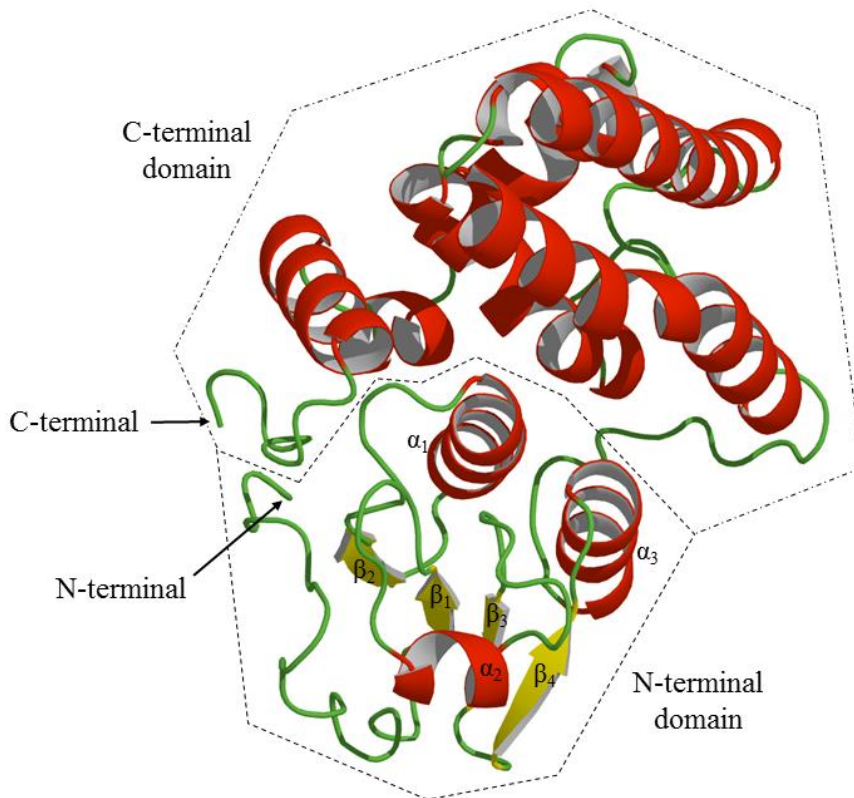

Fig. 8. The modeled tertiary structure of RfGSTρ. The strands, α helices and β sheets are represented in green lines, red coils and yellow arrows respectively.
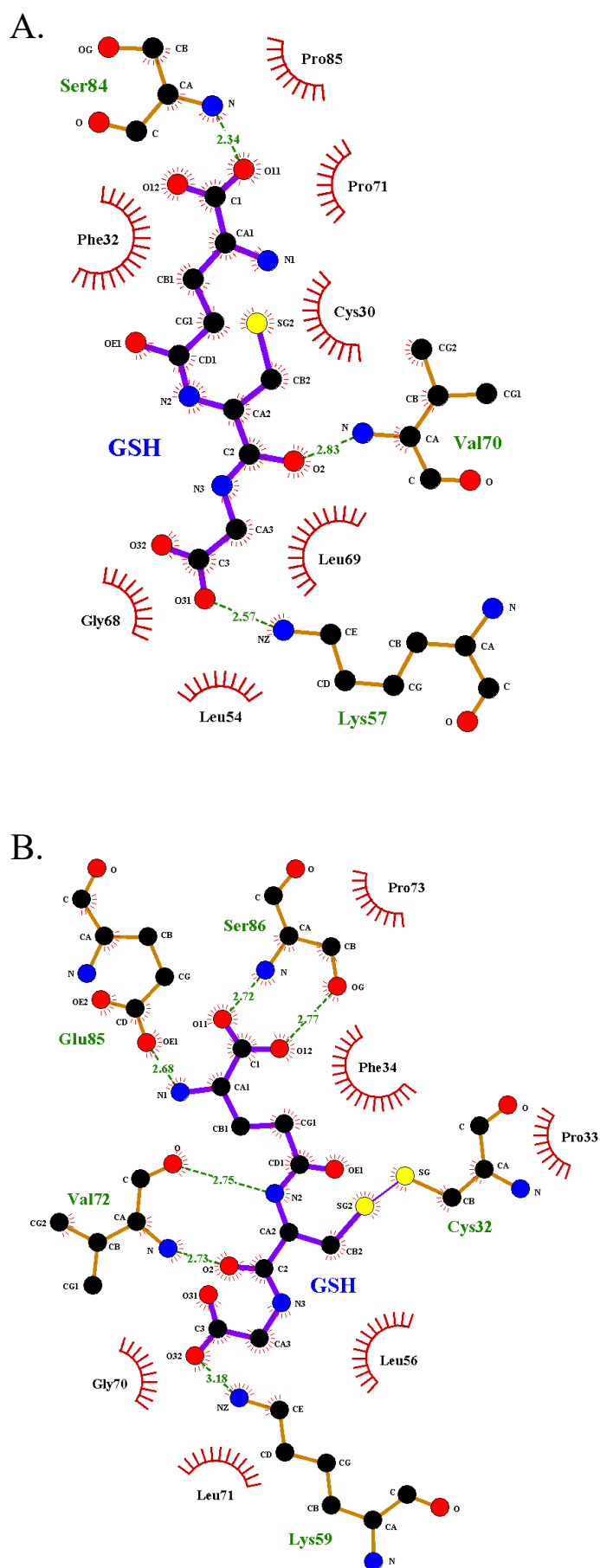
A.
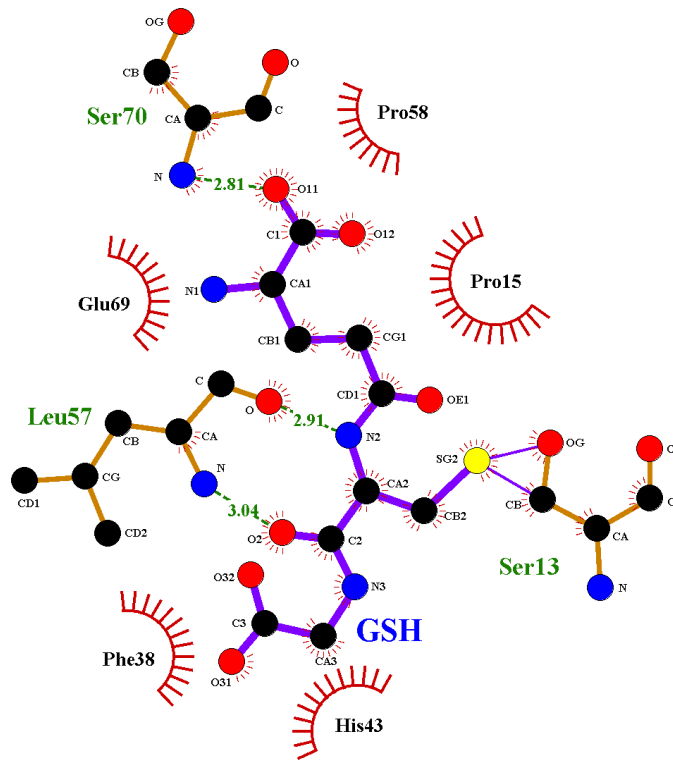
B.
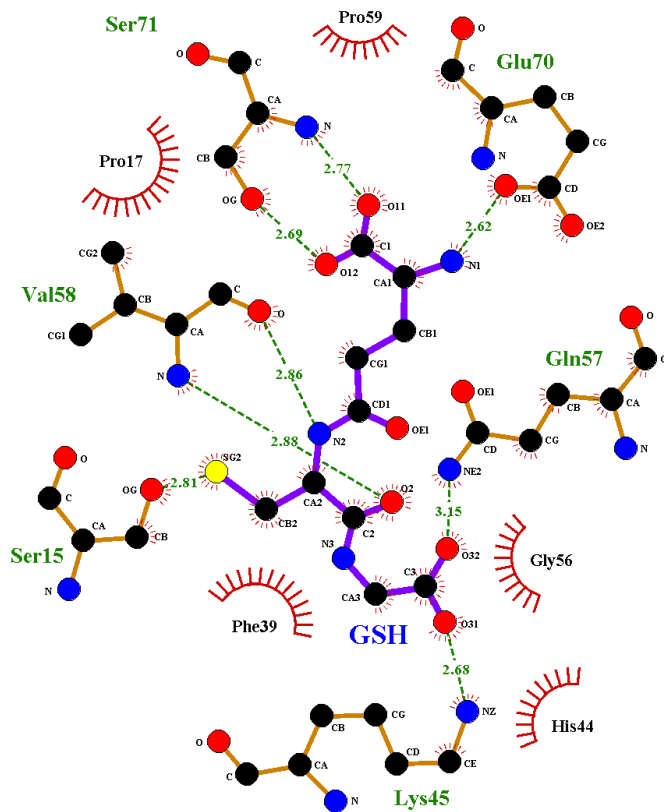
Fig. 9. Schematic illustration of the molecular interactions between amino acid residues in RfGSTρ (A) and LeGST (B)

The three dimensional model of RfGSTθ was fabricated using the crystal structure of human GST theta 1 (HsGSTθ; PDB entry 2c3t.1.A) which shared 53.95% identity and 45 % similarity (Fig. 10). GSH formed hydrogen bonds with Gln[10], Glu[64], Arg[105] and ligand bonds with Gln[51], Glu[64], Lys[234] of RfGSTθ (Fig. 11A). In the instance of HsGSTθ, GSH formed hydrogen bonds with Lys[41], Leu[54], Glu[66], Ser[67], Asp[104] and Arg[107] of HsGSTθ (Fig. 11B).
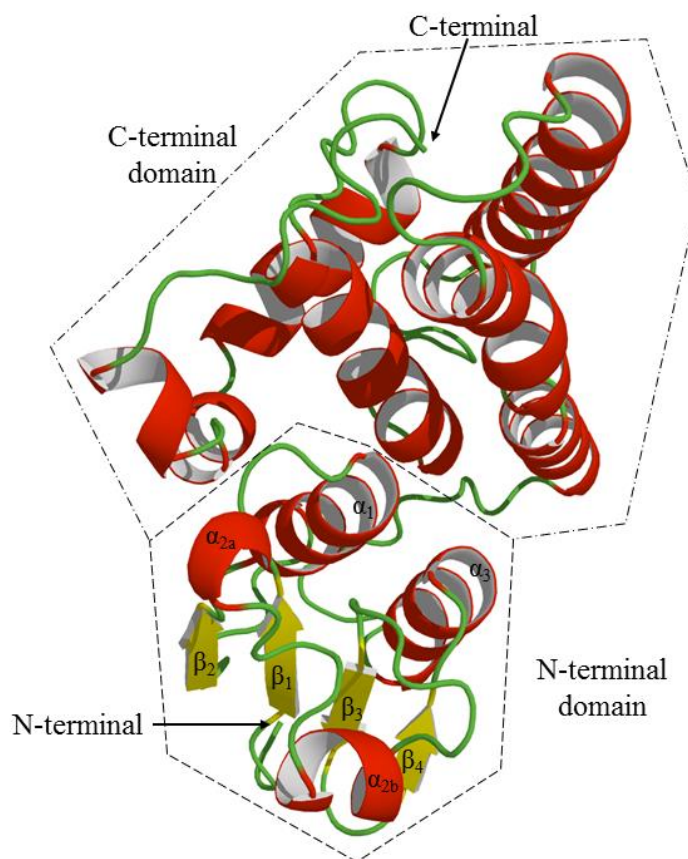

Fig. 10. The modeled tertiary structure of RfGSTθ. The strands, α helices and β sheets are represented in green lines, red coils and yellow arrows respectively.

A.

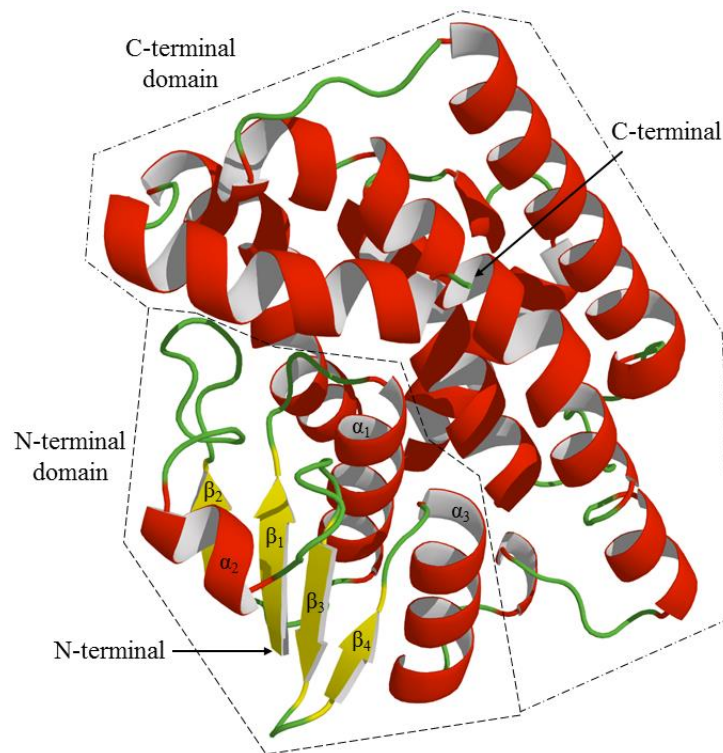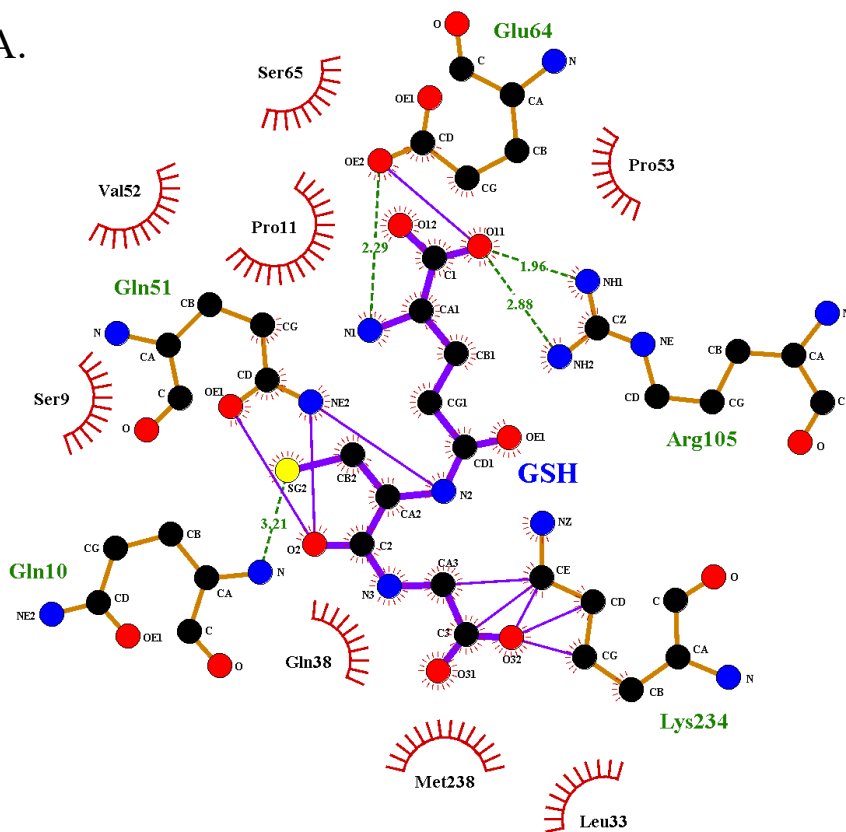B.
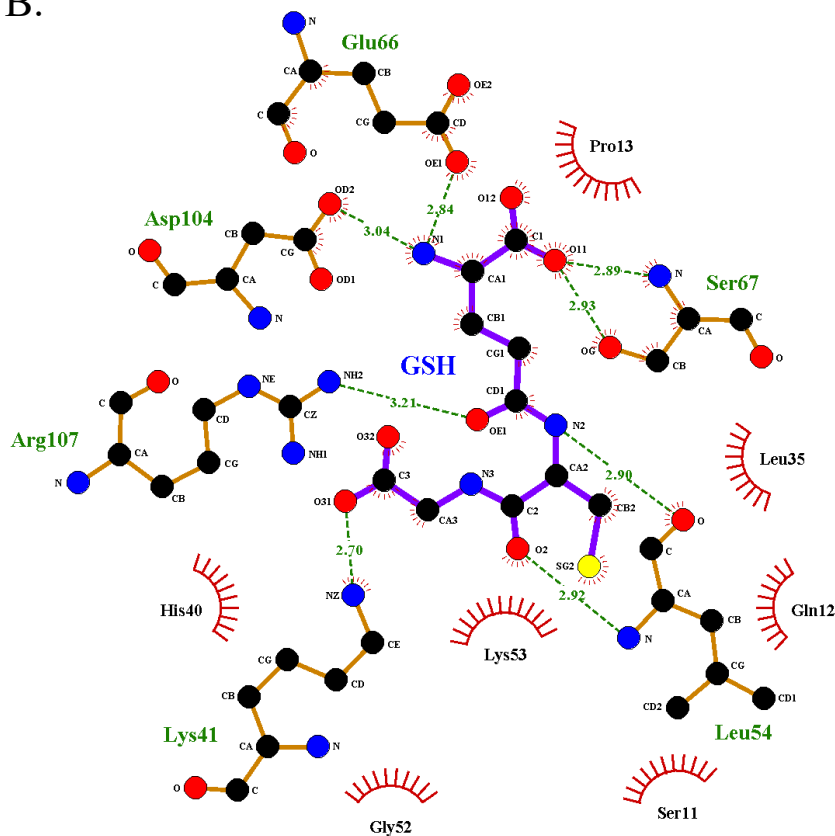
Fig. 11. Schematic illustration of the molecular interactions between amino acid residues in RfGSTθ (A) and HsGSTθ (B)

3.5 Expression, purification and biochemical characterization of fusion proteins

The ORFs of each three paralogs were cloned into pMAL-c5X respectively and overexpressed in *E. coli* ER2523. The fused proteins with maltose binding protein (MBP); rRfGSTω, rRfGSTρ and rRfGSTθ were purified separately and confirmed using the SDS-PAGE analysis (Fig 12). The biochemical properties of each protein and MBP protein were analyzed using common functional assays. The MBP tag of rRfGSTω was cleaved using the factor Xa (bovine plasma, Novagen) prior the analysis for the biochemical properties. However, the MBP tag was not cleaved from rRfGSTρ and rRfGSTθ, since, the activity of MBP towards each substrate was negligible, compared to the fusion protein.
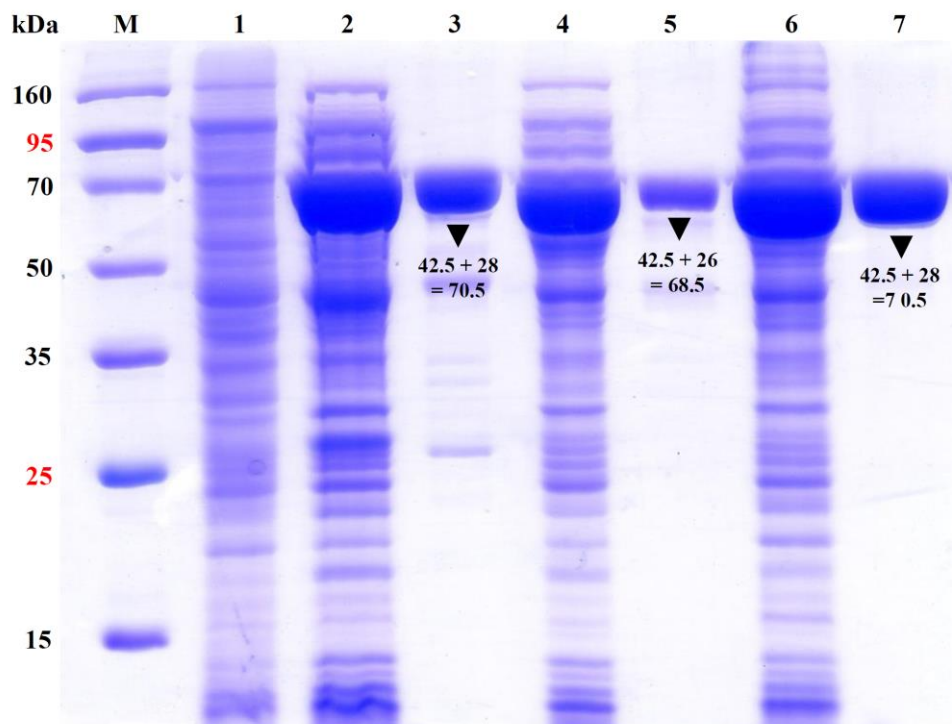
Fig. 12. SDS-PAGE of purified proteins. Samples were separated on 12% polyacrylamide gel. M: Protein maker (kDa). Lane 1: Total cellular extraction of *E. coli* ER2523 prior IPTG induction. Lane 2: Soluble portion of protein after IPTG induction. Lane 3: Purified fusion protein of RfGSTω/MBP (rRfGSTω). Lane 4: Soluble portion of protein after IPTG induction. Lane 5: Purified fusion protein of RfGSTρ/MBP (rRfGSTρ). Lane 6: Soluble portion of protein after IPTG induction. Lane 7: Purified fusion protein of RfGSTθ/MBP (rRfGSTθ).

31

3.5.1 Specific activity and kinetics

The specific activities of rRfGSTω, rRfGSTρ and rRfGSTθ towards several substrates were analyzed (Table 3). The rRfGSTω protein exhibited a detectable activity only towards DHA (0.36 $\pm$ 0.01 µmol min^{-1} mg^{-1}, n = 3), while both rRfGSTρ and rRfGSTθ showed detectable activities only towards CDNB (1.56 $\pm$ 0.01 µmol min^{-1} mg^{-1} and 2.05 $\pm$ 0.01 µmol min^{-1} mg^{-1}, n = 3, respectively). For further activities, DHA was selected as the respective substrate in the instance of rRfGSTω while CDNB was selected for both rRfGSTρ and rRfGSTθ.

When the GSH concentration was fixed, the K_m and V_max values were 33.62 $\pm$ 2.05 mM and 18.04 $\pm$ 0.4 mM, respectively in the kinetic assay conducted with rRfGSTω where DHA was used as the substrate. For the same assay conducted with rRfGSTρ using CDNB as the substrate, the K_m and V_max values were 3.02 $\pm$ 0.08 mM and 3.40 $\pm$ 0.09 mM respectively, while with rRfGSTθ the K_m and V_max values were 2.63 $\pm$ 0.04 mM and 15.80 $\pm$ 1.00 mM, respectively where CDNB was the substrate.

When the substrate concentration was fixed, the K_m and V_max values were 0.97 $\pm$ 0.14 mM and 2.02 $\pm$ 0.14 mM respectively in the kinetic assay conducted with rRfGSTω where DHA was the substrate. For the same assay conducted with rRfGSTρ using CDNB as the substrate, the K_m and V_max values were 14.10 $\pm$ 0.25 mM and 11.28 $\pm$ 0.70 mM, respectively while with rRfGSTθ the K_m and V_max values were 1.40 $\pm$ 0.15 mM and 10.01 $\pm$ 0.75 mM, respectively where CDNB was the substrate.

Table 6. Specific activity, optimum temperature, optimum pH, kinetics and inhibitor IC_{50} values of three paralogs

Protein	Substrate	Specific activity (μmol min^{-1} mg protein^{-1})	Optimum temperature (°C)	Optimum pH	Kinetics				Inhibitors IC_{50} (μM)	
					GSH		Substarte			
					K_m	V_{max}	K_m	V_{max}	CB	Hematin
RfGSTω	DHA	0.36±0.01	40	8.5	33.62 ± 2.05	18.04 ± 0.4	0.97 ± 0.14	2.02 ± 0.14	0.11	0.004
RfGSTρ	CDNB	1.56 ± 0.01	40	7.5	3.02 ± 0.08	3.40 ± 0.09	14.10 ± 0.25	11.28 ± 0.70	7	0.1
RfGSTθ	CDNB	2.05 ± 0.01	20	7.5	2.63 ± 0.04	15.8 ± 1.00	1.40 ± 0.15	10.01 ± 0.75	0.52	0.049

33

3.5.2 Temperature, pH, and inhibitor effect towards activity

The optimum temperature (Fig. 13A) and the optimum pH (Fig. 13B) for the DHAR activity with rRfGSTω were 40 °C and 8.5, respectively. Optimum temperatures for the CDNB conjugation activity with rRfGSTρ and rRfGSTθ were 40 °C and 20 °C, respectively while the optimum pH value was 7.5 in both of the instances.
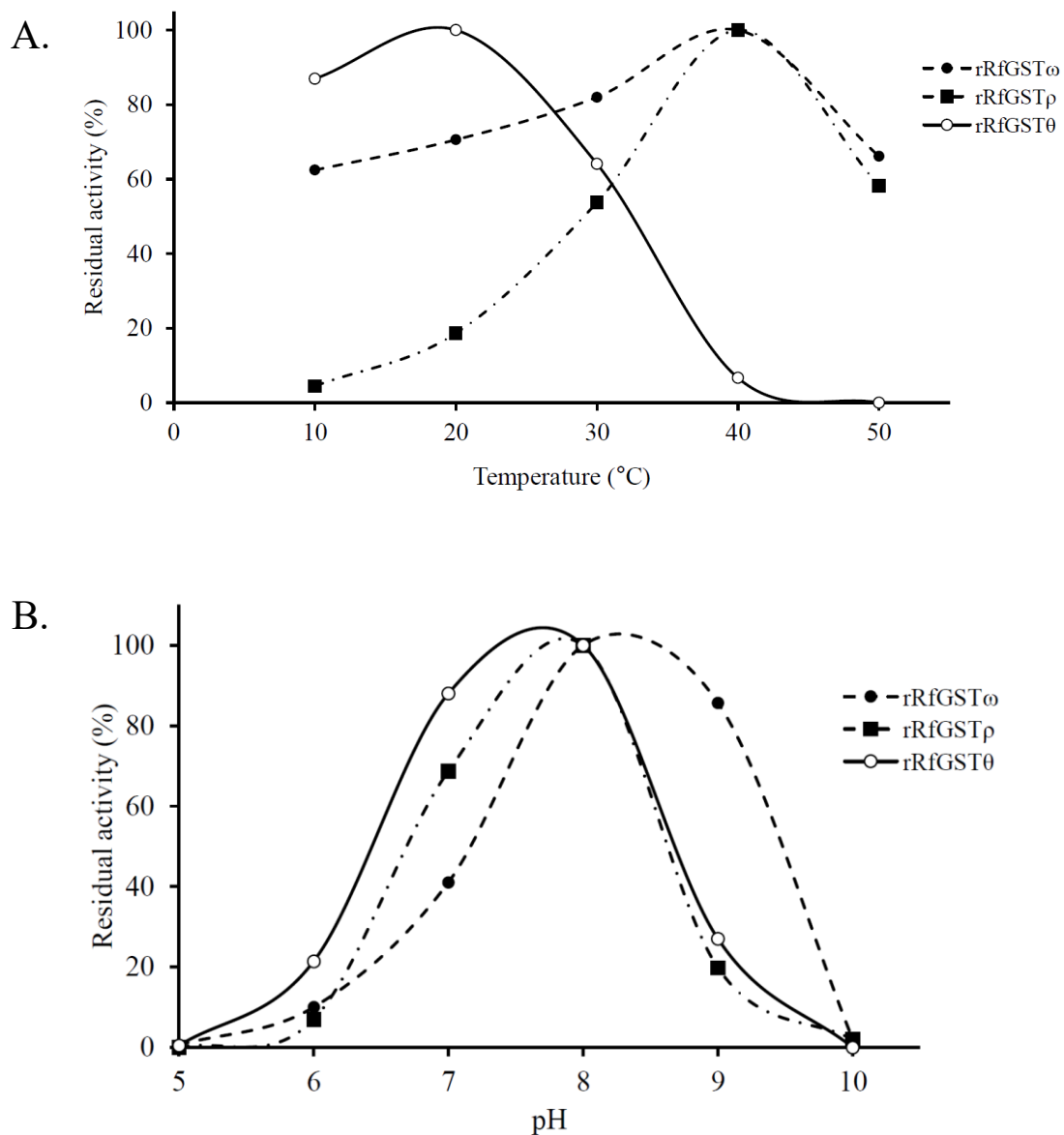
Fig. 13. Temperature (A), and pH (B) effect on the conjugating activity of three proteins (rRfGSTω, rRfGSTρ and rRfGSTθ).

In the inhibition assay (Fig. 14), CB exhibited 100% inhibition when the CB concentration was 1 μM towards DHAR activity of RfGSTω, while Hematin exhibited 98% inhibition at the same concentration. The IC_{50} values (Table 3) of the inhibition were 0.11 μM and 0.004 μM for CB and Hematin, respectively. Hundred percent inhibition of the DHAR activity with rRfGSTω was obtained at 10 μM of Hematin. The CDNB conjugation activity of rRfGSTρ was inhibited by 98% by 100 μM CB, while it was inhibited only by 68% at the same concentration of Hematin and the IC_{50} values of the inhibition were 7 μM and 0.1 μM for CB and Hematin, respectively. In the instance of CDNB conjugation activity of rRfGSTθ, CB unveiled 98% inhibition at 100 μM while 100% of inhibition was unveiled by Hematin at 10 μM of concentration and, the IC_{50} values of the inhibition were 0.52 μM and 0.049 μM for CB and Hematin, respectively.
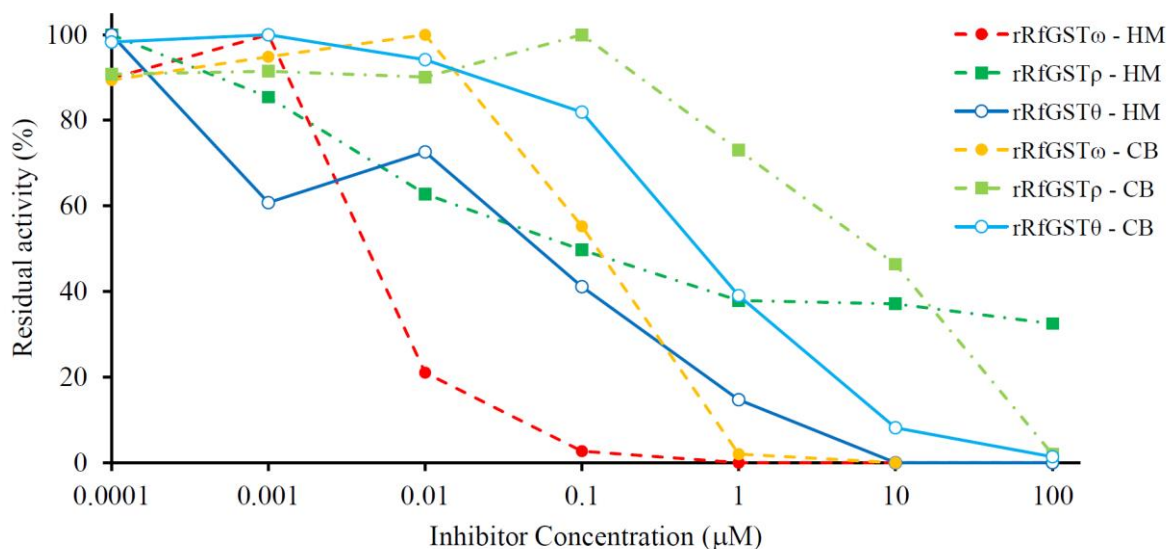

Fig. 14. Inhibitors effect on the conjugating activity of three proteins (rRfGSTω, rRfGSTρ and rRfGSTθ).

3.6   Disk diffusion study

3.6.1   Survival efficacy upon oxidative stress

Clearance zone was observed around the disks treated with 5 μL of H_2O_2 in all the bacteria plates with different magnitudes after incubation at 37 °C overnight (Fig. 15). The largest plaque with regard to H_2O_2 treatment could be observed in the u-EC plate (Fig. 15A) and the plaques observed in other bacteria plates were significantly reduced. Compared to the plaque diameter observed in v-EC plate (Fig. 15B) around the H_2O_2 treated disks, ω-EC (Fig. 15C) and θ-EC (Fig. 15E) were significantly reduced while the plaque diameter of ρ-EC (Fig. 15D) plate was not significantly different.

3.6.2   Survival efficacy upon heavy metals

Around the heavy metal treated disks, clearance zones were observed in all the bacteria plates in different magnitudes after incubation at 37 °C overnight (Fig. 15). With regard to $CdCl_2$ treated disks, the maximum plaque diameter was observed in u-EC plate. The plaque size was not significantly different in v-EC and ρ-EC plates while it was significantly reduced in ω-EC and θ-EC plates (Fig. 16). The maximum clearance zones were observed in u-EC and v-EC regarding the $CuSO_4$ treated disks. The plaque diameter was significantly reduced in other plates where the minimum diameter was recorded in ω-EC plate. The plaque diameter of all the plates were significantly reduced compared to the u-EC plate which was recorded with the maximum value with regard to $ZnCl_2$ treated disks. The plaque size in ω-EC, ρ-EC and θ-EC plates were significantly reduced than that of v-EC whereas the minimum value was observed in the ω-EC plate.
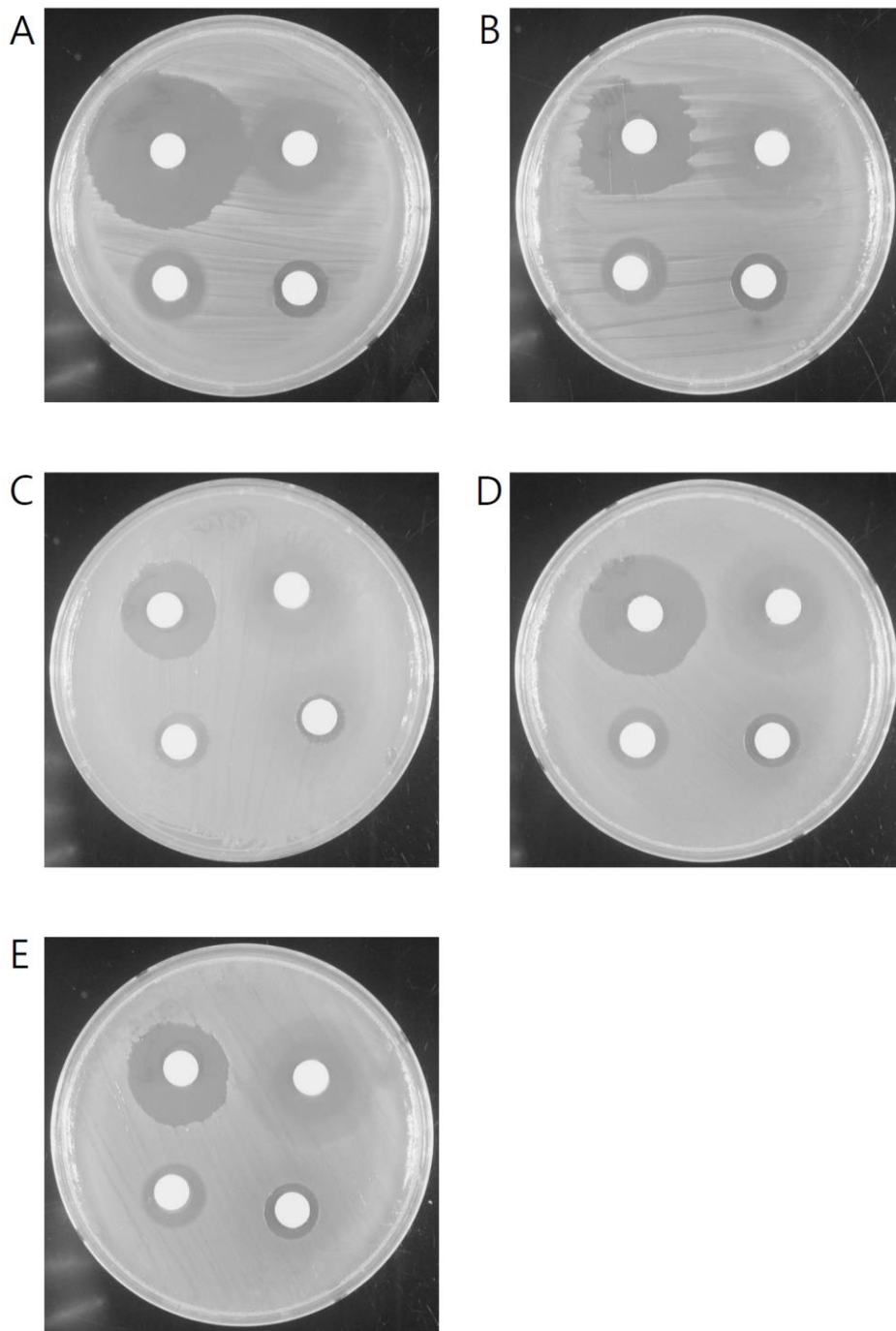
Fig. 15. Disk diffusion assay. Each disk was treated with 5 µL of respective chemical; upper Left – H$_2$O$_2$, upper right – CdCl$_2$, lower Left ZnCl$_2$ and lower right CuSO$_4$. A. untransformed *E. coli* (u-EC). B. transformed *E. coli* with only pMAL c5x vector (v-EC). C. Transformed *E. coli* with RfGSTω/MBP fusion vector (ω-EC). D. Transformed *E. coli* with RfGSTρ/MBP fusion vector (ρ-EC). E. Transformed *E. coli* with RfGSTθ/MBP fusion vector (θ-EC).
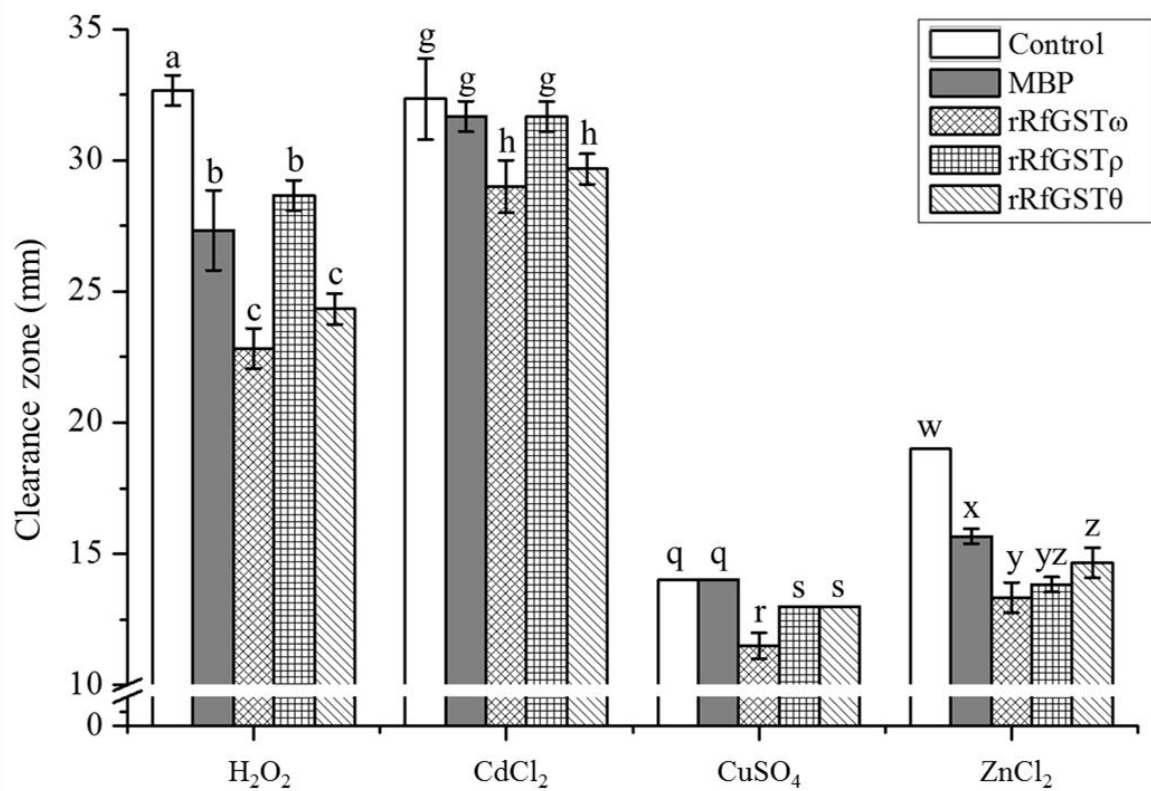
Fig. 16. Disk diffusion assay summary. Data are presented as mean (n = 3) ± SD. Data with different letters are significantly different among each group ($p < 0.05$).

3.7   The mRNA expression: quantitative analysis

All three paralogs (*RfGSTω*, *RfGSTρ* and *RfGSTθ*) were ubiquitously expressed in blood cells and all the tissues analyzed in the study namely; head kidney, spleen, liver, gill, intestine, kidney, heart, testis and ovary (Fig. 17). The highest mRNA expression of *RfGSTω* was detected in blood cells with ~222-fold difference to the least expressed tissue; intestine. Next to blood cells, the mRNA was highly expressed in liver and ovary tissues with 75-fold and 35-fold, respectively. The *RfGSTρ* paralog was depicted its highest expression level in the liver tissue where it scored 198-fold difference compared to the least expressed tissue; intestine. Testes and ovary expressed highly next to liver (39-fold and 26-fold, respectively). Liver tissue showed the highest mRNA expression level with 4780-fold compared to the least expressed tissue; ovary where testes and gill showed higher mRNA expression levels with 186-fold and 126-fold, respectively in the instance of *RfGSTθ*. The single peak in dissociation curve of each paralog and rockfish *RfEF1A* confirmed the specificity of each primer set.
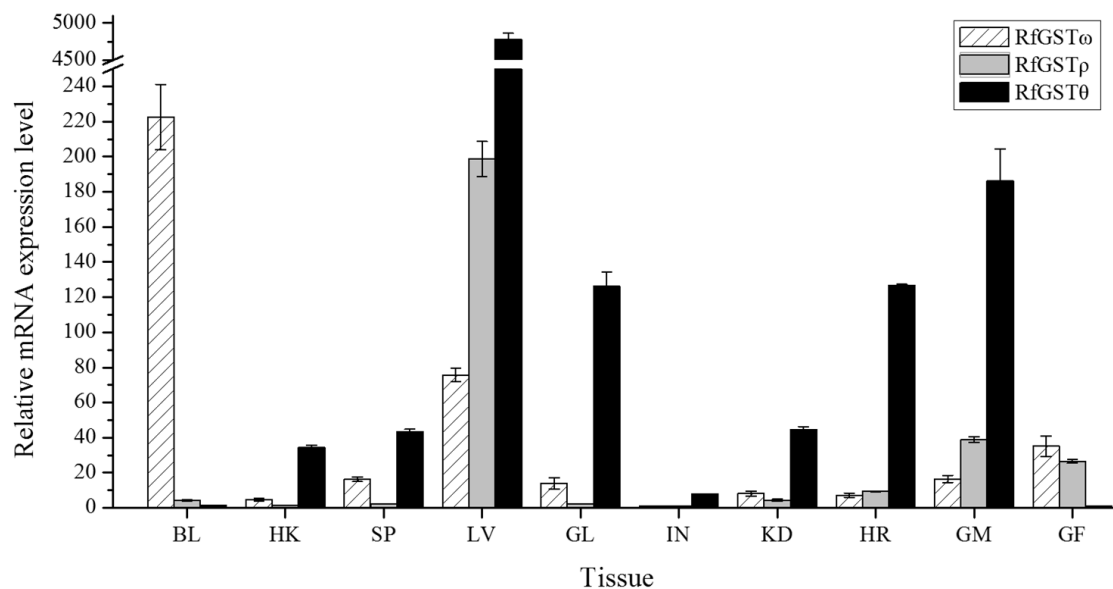
Fig. 17. Tissue specific transcriptional profile of three paralogs; BL, blood; HK, head kidney; SP, spleen; LV, liver; GL, gill; IN, intestine; KD, kidney; HR, heart; GM, testis; GF, ovary. Data are presented as mean (n = 3) ± SD.

Upon the *S. iniae* bacterial challenge (Fig. 18), *RfGSTω* mRNA level in blood was significantly ($P < 0.05$) elevated by 1.8-fold and 1.9-fold at 3 hours post injection (h.p.i) and 6 h.p.i., respectively. After 6 h.p.i., the mRNA level was drastically reduced and achieved its control level at 12 h.p.i. and retained thereafter. *RfGSTρ* mRNA expression level in liver tissue was significantly down-regulated at the early phase of the bacterial infection and, leveled up at 12 h.p.i. to the control level. Interestingly, after 12 h.p.i., mRNA level was drastically down-regulated. Significant up-regulation of *RfGSTθ* mRNA expression in liver tissue was observed at all the time points except at 24 h.p.i. where a significantly down-regulated mRNA level was detected.

Fig. 18. Expression analysis after challenge experiments with *S. iniae* carried out by qPCR. Data are expressed as mean fold-induction (n = 3) relative to the PBS control ± SD. Data with different letters are significantly different among each group ($p < 0.05$). Blood tissue of *RfGSTω* and liver tissue of *RfGSTρ* and *RfGSTθ* were investigated in each challenge experiment.

Poly I:C challenge experiment results (Fig. 19) revealed that, *RfGSTω* mRNA level in blood could be significantly up-regulated by viral stimuli. The highest mRNA transcription was observed at 6 h.p.i. with ~3-fold difference. *RfGSTρ* mRNA expression level in liver tissue shown a fluctuated pattern with significant down-regulations and control levels. Up to 6 h.p.i., *RfGSTθ* mRNA expression in liver tissue was at the control level. After a significant down-regulation at 12 h.p.i., the mRNA expression level of *RfGSTθ* was elevated significantly, and achieved its highest mRNA level at 48 h.p.i (1.7-fold).
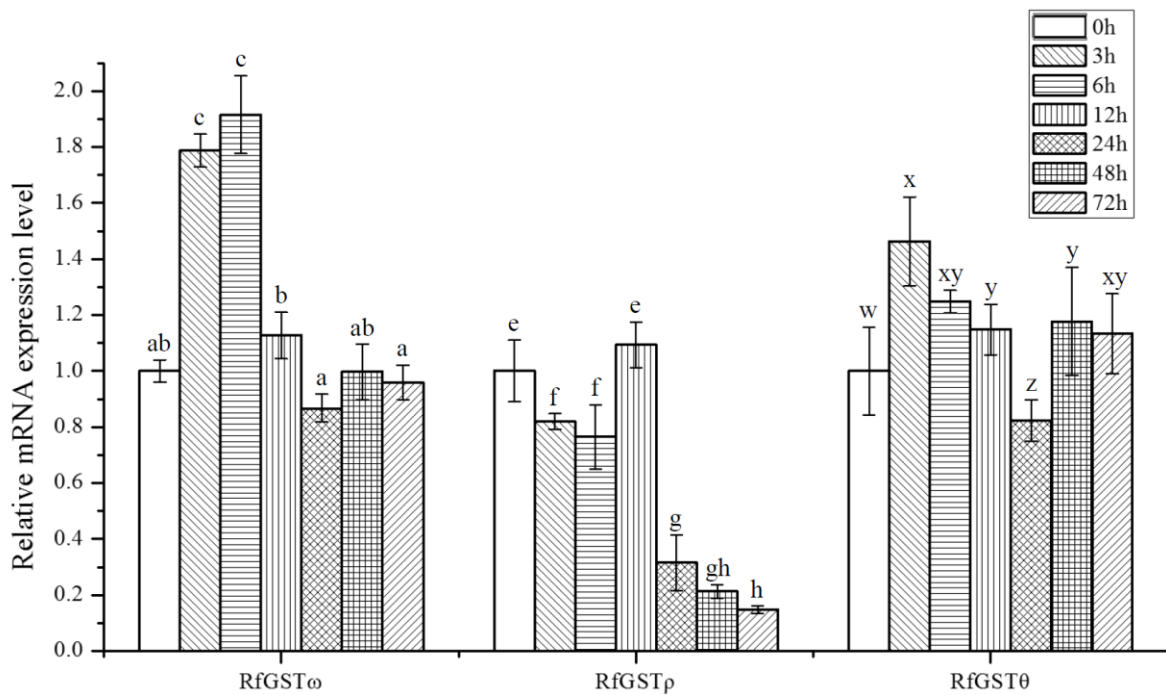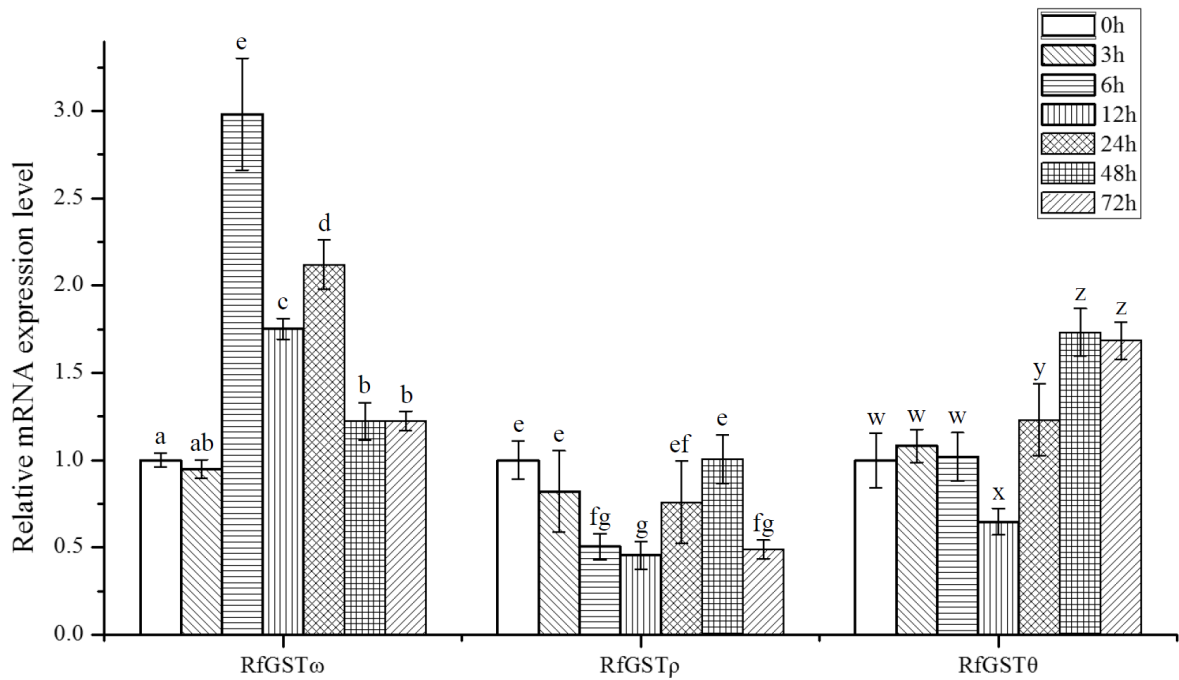

Fig. 19. Expression analysis after challenge experiments with Poly (I:C) carried out by qPCR. Data are expressed as mean fold-induction (n = 3) relative to the PBS control ± SD. Data with different letters are significantly different among each group ($p < 0.05$). Blood tissue of *RfGSTω* and liver tissue of *RfGSTρ* and *RfGSTθ* were investigated in each challenge experiment.

4. DISCUSSION

GSTs are comprised of a common structure with two domains namely the N-terminal domain (domain I) which entails both α helices and β strands, and the C-terminal domain (domain II) with 4-7 α helices (Frova, 2006). Domain I contains thioredoxin like fold (βαβαββα) which can be clearly separated into two typical structural motifs as N-terminal $\beta_1\alpha_1\beta_2$ and C-terminal $\beta_3\beta_4\alpha_3$ (Frova, 2006). The motifs are linked together with a long loop consisting of an α-helix (α_2). Interestingly, RfGSTρ is slightly deviated from the common architecture comprising two α sheets (α_{2a} and α_{2b}) in between β_2 and β_3 strands (Fig 1B). This may be due to GSTρ paralogs are restricted to the aquatic organisms and they might be evolved differently than that of other paralogs. The highly conserved *cis*-Proline was identified at α_2 and β_3 connecting loop of three paralogs as depicted in GST family proteins which indeed important to maintain the proper confirmation of the enzyme fold (Allocati et al., 1999; Frova, 2006). The residue was found to be an important for the catalytic function and stability of thioredoxin-like proteins whereas the mutation studies have proven its importance in the catalytic function, conformational stability as well as the function as an antibiotic binding determinant (Allocati et al., 1999; Nathaniel et al., 2003).

At the active site, GSTω orthologs encompass Cys residue in the place of Ser or Tyr which can be found in the other GST classes which forms the disulfide bond with GSH (Sheehan et al., 2001). The Cys residue promotes mixed disulphide formation other than the formation of thiolate anion (Frova, 2006). The same eccentric is shared by beta class GST, lambda class GST, DHAR, glutaredoxin and chloride intracellular channel protein (CLIC). The conserved active Cys residue in RfGSTω was found to be Cys[30] which unlike in human GSTω, was formed a hydrophobic interaction with GSH in the place of the hydrogen bond (Board et al., 2000). Binding energy which undeniably important for the molecular recognition and

interactions of a protein is delimited by charge-charge interactions, hydrogen bonding and hydrophobic interactions in aqueous solution (Fersht, 1999). Therefore, activities of two orthologs may be different from each other as they achieve conformities with xenobiotics via different mechanisms. At the active site, GSTρ orthologs contain a Ser residue as depicted in OlfGST rho and in many GST family proteins whereas in RfGSTρ, Ser[15] was the active moiety (Sheehan et al., 2001; Espinoza et al., 2013). In comparison, LeGST, Ser[15] residue forms a hydrogen bond with the S atom of GSH while in RfGSTρ, C and O atoms of corresponding Ser[13] residue forms two ligand bonds with the S atom of GSH (Park et al., 2013). Additionally, higher bonding aptitude was revealed by GSH with LeGST than that of RfGSTρ further demonstrating their conformational deviation on the other hand, evidencing their functional variation (Fig. 3C and 3D).   GSTθ paralogs are supposed to have a Ser residue other than Tyr residue present in alpha, mu and pi class GSTs as their active site which supposed to active the GSH substrate (Blocki et al., 1993; Board et al., 1995; Wilce et al., 1995). The active Ser residue of RfGSTθ can be identified as Ser[9] which is highly conserved among other GSTθ orthologs (Rossjohn et al., 1996). The putative role for Ser has been observed to be the stabilization and promotion of the thiolate anion and its importance has been confirmed by the site-directed mutagenesis (Board et al., 1995). However, the active Ser of GSTθ was found to be buried and additionally it appears to have a purpose-built sulfate-binding site (Rossjohn et al., 1998). In the comparison of GSTθ orthologs, RfGSTθ showed comparatively complicated bonding pattern than that of human GSTθ. However, in both proteins, the active moiety Ser residue formed hydrophobic interactions with GSH.

GSTρ counterparts are in a controversial state among the species specificity. Some studies reported that GSTρ is a fish specific GST family protein (Konishi et al., 2005; Liang et al., 2007), while in other studies reported them as mollusks specific GST family protein (Park et al., 2013). Additionally, *Branchiostoma belcheri* an amphioxus was reported to present a

GSTρ ortholog which shared almost alike identities and similarities with both kinds; fish and mollusks (Fan et al., 2007) (Supplementary table). The present results revealed that, the mollusks shared less than 50% identities and less than 70% similarities with fish counterparts where they shared identities over 70% and similarities over 80% with RfGSTρ though they were claded in the same cluster. However, further studies are required to be done in order to understand the real species specificity of GSTρ.

CDNB has been identified as the universal GST substrate (Board et al., 2000). Though some GSTω counterparts exhibited activity towards CDNB, rRfGSTω did not show any countable activity towards CDNB with the presence of GSH (Board et al., 2000; Rhee et al., 2008). From the chemicals used in our study, rRfGSTω was exhibited satisfactory activity only towards DHA similarly to *H. discus discus* (Wan et al., 2009) and *D. rerio* (Glisic et al., 2015) GSTω counterparts. Both of the other paralogs (rRfGSTρ and rRfGSTθ) exhibited countable activities only towards CDNB. Despite *P. major* GSTρ (pmGSTR1-1) (Konishi et al., 2005) was exhibited alike pattern towards each substrate, *B. belcheri* GSTρ (Fan et al., 2007) counterpart exhibited countable activity with ECA in addition to CDNB. GSTθ counterpart of *Bombyx mori* also exhibited detectable activities towards ECA (Yamamoto et al., 2005) while rRfGSTθ did not show any countable activity with ECA. Interestingly, rRfGSTω achieved its highest DHAR activity potential at comparatively higher temperature (40 °C) bestowing its higher temperature adaptability. No previous studies on temperature stability of fish GSTω counterparts were reported up to date. However, a molluscan GSTω counterpart from *H. discus discus* (rAbGSTω) showed its highest DHAR activity potential at 25 °C (Wan et al., 2009). Optimum pH for the DHAR activity of rRfGSTω (pH 8.5) did not exhibited contrast deviation from other orthologs, whereas rAbGSTω and *Schistosoma mansoni* GSTω counterparts exhibited their optimum DHAR activity at pH 8 (Girardini et al., 2002; Wan et al., 2009). The maximum temperature as well as the optimum pH of the CDNB conjugation activity of

rRfGSTρ was higher than that of pmGSTR1-1 (Konishi et al., 2005). CDNB conjugation activity of rRfGSTθ ortholog acquired its maximum potential at a lower temperature (20 °C) than that of other GSTθ counterparts, whereas *Neanthes succinea* GSTθ exhibited its highest potent temperature for the CDNB conjugation activity at 37 °C (Rhee et al., 2007), while *B. mori* GSTθ at 40 °C (Yamamoto et al., 2005). However, optimum pH values seems quite varied among GSTθ counterparts (Yamamoto et al., 2005; Rhee et al., 2007). Interestingly, neither temperature studies nor pH studies were conducted with teleost GSTθ counterparts so far. Our results implicated that rRfGST paralogs achieve their maximum proximities towards respective activities in diverse temperature and pH values intraspecifically as well as interspecfically. However, more studies with other teleosts should be carried out for a better comparison.

Inhibition assays can be conducted to distinguish the isozymes or differentiate enzyme species (Mannervik and Danielson, 1988). To investigate the comportment of our GST paralogs towards different inhibitors, inhibitory assays were conducted with CB and hematin which have been identified as effective inhibitors of GSTs in previous studies (Mannervik and Danielson, 1988). In the present study, inhibitor concentration gradient was prepared from 0.0001 μM to 100 μM, and inhibitory potential was determined upon respective activities. Hematin showed higher inhibitory potential than CB with respective to IC_{50} values in all the instances. The same consequence could be observed with *N. succinea* GSTω and *R. marmoratus* GSTθ counterparts (Lee et al., 2006; Rhee et al., 2008) nonetheless, CB was recorded with higher inhibitory potential in the instance of *N. succinea* GSTθ (Rhee et al., 2007). Up to date, none of the reports were found with inhibition studies of GSTρ counterparts. Interestingly, rRfGSTρ shows somewhat similar response towards CB and hematin to previously reported GSTα with respect to IC_{50} values (Mannervik et al., 1985). Inhibitory potential was varied with the paralog restating their functional differences.

The cell protection potential of GSTs upon oxidative stress generated by H_2O_2 has been

45

well documented (Fiander and Schneider, 1999; Singhal et al., 1999; Yang et al., 2001; Kanai et al., 2006). Disk diffusion assay strongly demonstrated that the GSTs have enabled *E. coli* to overcome oxidative stress and survive efficiency than u-EC as well as v-EC in the instances of ω-EC and θ-EC. Interestingly, ρ-EC was futile in the efficacy of protecting *E. coli* from oxidative stress. Previous study with sigma class GST of teleost counterpart has revealed their potency to protect bacterial cells from oxidative stress (Lee et al., 2007). Collectively, it can be suggested that bacterial cells incorporated with GSTs have potent to overcome the oxidative stress in a competitive magnitude.

Cadmium is a predominant in the environment yet non-essential, highly toxic chemical to living organisms (Muthukumar and Nachiappan, 2010). Copper a redox-active heavy metal catalyzes the hydroxyl radical formation via Haber-Weiss reaction and develop oxidative stress to the living cells while Cadmium and Zinc like heavy metals short of redox potential, inactivate the cellular antioxidants interrupting the metabolic balance (Stohs and Bagchi, 1995; Tripathi and Gaur, 2004). Collectively, heavy metals generate oxidative stress to the living cells. To investigate whether our GSTs grant the protection upon oxidative stress mediated by heavy metals to the *E. coli* cells, disk diffusion assay was conducted. Interestingly, the clearance zone around $CdCl_2$ treated disks was not clearly defined with the distance since the bacterial growth might be retarded with the increased diameter than killing the bacteria. The clearance zones in ω-EC and θ-EC plates were significantly reduced in all the instances than that of both u-EC and v-EC showing GSTω and GSTθ have protected the *E. coli* cells from the stress generated by the heavy metals in a significant level. Though, GSTρ was futile to offer survival potential to the *E. coli* cells upon Cd, in the instances of Cu and Zn, significant survival protection was observed. However, *in-vivo* studies to be carried out as a future direction for a better conclusion remark.

The spatial distribution of GST paralogs among tissues was assessed using SYBR green

qPCR analysis. The single peak in dissociation curve of each GST paralog and *RfEF1α* confirmed the specificity of each primer set. Out of three paralogs, two paralogs; *RfGSTρ* and *RfGSTθ* were recorded their highest mRNA expression level in liver nevertheless, *RfGSTω* was expressed in liver in a significant magnitude. Similarly, higher mRNA expression was observed in liver tissue of *D. rerio* with regard to *RfGSTρ*, *RfGSTθ* and yet, *RfGSTω* mRNA expression was minute (Glisic et al., 2015). Though, *RfGSTω* was mainly expressed in blood, the mRNA expression of other orthologs in blood was significantly low. Since the genes were expressed highly in blood and liver, mRNA expression upon bacterial and viral stimuli was investigated in those two tissues. For the challenge experiment with bacteria, *S. iniae* a gram positive bacteria which has been identified as one of the most serious pathogen in finfish aquaculture was selected (Agnew and Barnes, 2007). For the viral challenge experiment with black rockfish, poly (I:C), a synthetic double-stranded RNA used in model viral infections was selected (Fortier et al., 2004). However, significant variation could not be observed in liver in regard to *RfGSTω* and blood in regard to *RfGSTρ* and *RfGSTθ* paralogs (data not shown). Hence, for the study, blood was selected for *RfGSTω* and liver was selected for other two paralogs, *RfGSTρ* and *RfGSTθ*. Upon *S. iniae* stimulus, *RfGSTω* and *RfGSTθ*, paralogs had shown slight yet significant up-regulation at the early stage of the invasion. However, with the time, the mRNA level was achieved the level of control in the instance of *RfGSTω*, while in *RfGSTθ* mRNA level was fluctuated around the control level. In contrast, *RfGSTρ* demonstrated significant down-regulation upon the bacterial stimulus which may be due to the mRNA turnover effect (Mitchell and Tollervey, 2001). Upon poly (I:C) stimulus, *RfGSTω* showed comparably higher up-regulation at the early stage while *RfGSTθ* showed up-regulation at the latter part of the experimental period. However, *RfGSTρ* exhibited the same down-regulation pattern of bacterial challenge but, in a fluctuated manner. Interestingly, no studies have been conducted to investigate GSTs mRNA regulation under pathogenic stress in fish au courant. However, the

studies with GST paralogs in different organisms have been proved their conceivable protective

aptitudes from pathogenic stress as well (Saranya Revathy et al., 2012; Umasuthan et al., 2012;

Bathige et al., 2014).

5. CONCLUSION

Our study conferred a comprehensive analysis of three GST family proteins; GSTω, GSTρ, and GSTθ from black rockfish. All three paralogs revealed their common domain architecture though they were slightly diverged from their corresponding orthologs in respect to activities, active moieties and GSH binding pocket architectures. Their enzymatic activities towards respective substrates, activities under different temperatures and pH values, kinetic parameters as well as inhibitory potential generated by known GST inhibitors reveled their functional variation and validated their existence as paralogs. Additionally, we have revealed the protective dimensions of our three paralogs against oxidative stress and heavy metals such as Cd, Cu and Zn *in vitro*. Since their mRNA expressional modulation appeared in higher magnitudes, we suggest their involvement in innate immunity and the axiom was reinforced by the up-regulated expression of mRNA in respect to *RfGSTω* and *RfGSTθ* paralogs under pathogenic stress. Collectively, our findings deliver the broadened scopes of GSTω, GSTρ, and GSTθ paralogs from teleost species opening new dimensions for further studies with GST paralogs.

REFERENCES

Agnew, W. and Barnes, A.C., 2007. Streptococcus iniae: an aquatic pathogen of global veterinary significance and a challenging candidate for reliable vaccination. Vet Microbiol 122, 1-15.

Allocati, N., Casalone, E., Masulli, M., Ceccarelli, I., Carletti, E., Parker, M.W. and Di Ilio, C., 1999. Functional analysis of the evolutionarily conserved proline 53 residue in Proteus mirabilis glutathione transferase B1-1. FEBS Lett 445, 347-50.

Balendiran, G.K., Dabur, R. and Fraser, D., 2004. The role of glutathione in cancer. Cell Biochem Funct 22, 343-52.

Bathige, S.D., Umasuthan, N., Saranya Revathy, K., Lee, Y., Kim, S., Cho, M.Y., Park, M.A., Whang, I. and Lee, J., 2014. A mu class glutathione S-transferase from Manila clam Ruditapes philippinarum (RpGSTmu): cloning, mRNA expression, and conjugation assays. Comp Biochem Physiol C Toxicol Pharmacol 162, 85-95.

Blocki, F.A., Ellis, L.B. and Wackett, L.P., 1993. MIF protein are theta-class glutathione S-transferase homologs. Protein Sci 2, 2095-102.

Board, P.G., Coggan, M., Chelvanayagam, G., Easteal, S., Jermiin, L.S., Schulte, G.K., Danley, D.E., Hoth, L.R., Griffor, M.C., Kamath, A.V., Rosner, M.H., Chrunyk, B.A., Perregaux, D.E., Gabel, C.A., Geoghegan, K.F. and Pandit, J., 2000. Identification, characterization, and crystal structure of the Omega class glutathione transferases. J Biol Chem 275, 24798-806.

Board, P.G., Coggan, M., Wilce, M.C. and Parker, M.W., 1995. Evidence for an essential serine residue in the active site of the Theta class glutathione transferases. Biochem J 311 (Pt 1), 247-50.

Bradford, M.M., 1976. A rapid and sensitive method for the quantitation of microgram quantities of protein utilizing the principle of protein-dye binding. Anal Biochem 72, 248-54.

Calvin, H.I., Hwang, F.H. and Wohlrab, H., 1975. Localization of zinc in a dense fiber-connecting piece fraction of rat sperm tails analogous chemically to hair keratin. Biol Reprod 13, 228-39.

Dixon, D.P., Davis, B.G. and Edwards, R., 2002. Functional divergence in the glutathione transferase superfamily in plants. Identification of two classes with putative functions in redox homeostasis in Arabidopsis thaliana. J Biol Chem 277, 30859-69.

Droege, M. and Hill, B., 2008. The Genome Sequencer FLX System--longer reads, more

applications, straight forward bioinformatics and more complete data sets. J Biotechnol 136, 3-10.

Espinoza, H.M., Shireman, L.M., McClain, V., Atkins, W. and Gallagher, E.P., 2013. Cloning, expression and analysis of the olfactory glutathione S-transferases in coho salmon. Biochem Pharmacol 85, 839-48.

Fan, C., Zhang, S., Liu, Z., Li, L., Luan, J. and Saren, G., 2007. Identification and expression of a novel class of glutathione-S-transferase from amphioxus Branchiostoma belcheri with implications to the origin of vertebrate liver. Int J Biochem Cell Biol 39, 450-61.

Fersht, A., 1999. Structure and mechanism in protein science: a guide to enzyme catalysis and protein folding, W. H. Freeman and Company, United States of America.

Fiander, H. and Schneider, H., 1999. Compounds that induce isoforms of glutathione S-transferase with properties of a critical enzyme in defense against oxidative stress. Biochem Biophys Res Commun 262, 591-5.

Fortier, M.E., Kent, S., Ashdown, H., Poole, S., Boksa, P. and Luheshi, G.N., 2004. The viral mimic, polyinosinic:polycytidylic acid, induces fever in rats via an interleukin-1-dependent mechanism. Am J Physiol Regul Integr Comp Physiol 287, R759-66.

Frova, C., 2006. Glutathione transferases in the genomics era: new insights and perspectives. Biomol Eng 23, 149-69.

Girardini, J., Amirante, A., Zemzoumi, K. and Serra, E., 2002. Characterization of an omega-class glutathione S-transferase from Schistosoma mansoni with glutaredoxin-like dehydroascorbate reductase and thiol transferase activities. Eur J Biochem 269, 5512-21.

Glisic, B., Mihaljevic, I., Popovic, M., Zaja, R., Loncar, J., Fent, K., Kovacevic, R. and Smital, T., 2015. Characterization of glutathione-S-transferases in zebrafish (Danio rerio). Aquat Toxicol 158, 50-62.

Hayes, J.D. and Pulford, D.J., 1995. The glutathione S-transferase supergene family: regulation of GST and the contribution of the isoenzymes to cancer chemoprotection and drug resistance. Crit Rev Biochem Mol Biol 30, 445-600.

Hwang, H.K., Son, M.H., Myeong, J.I., Kim, C.W. and Min, B.H., 2014. Effects of stocking density on the cage culture of Korean rockfish (Sebastes schlegeli). Aquaculture 434, 303-306.

Kanai, T., Takahashi, K. and Inoue, H., 2006. Three distinct-type glutathione S-transferases from Escherichia coli important for defense against oxidative stress. J Biochem 140,

703-11.

Konishi, T., Kato, K., Araki, T., Shiraki, K., Takagi, M. and Tamaru, Y., 2005. A new class of glutathione S-transferase from the hepatopancreas of the red sea bream Pagrus major. Biochem J 388, 299-307.

Lee, Y.M., Lee, K.W., Park, H., Park, H.G., Raisuddin, S., Ahn, I.Y. and Lee, J.S., 2007. Sequence, biochemical characteristics and expression of a novel Sigma-class of glutathione S-transferase from the intertidal copepod, Tigriopus japonicus with a possible role in antioxidant defense. Chemosphere 69, 893-902.

Lee, Y.M., Seo, J.S., Jung, S.O., Kim, I.C. and Lee, J.S., 2006. Molecular cloning and characterization of theta-class glutathione S-transferase (GST-T) from the hermaphroditic fish Rivulus marmoratus and biochemical comparisons with alpha-class glutathione S-transferase (GST-A). Biochem Biophys Res Commun 346, 1053-61.

Liang, X.F., Li, G.G., He, S. and Huang, Y., 2007. Transcriptional responses of alpha- and rho-class glutathione S-transferase genes in the liver of three freshwater fishes intraperitoneally injected with microcystin-LR: relationship of inducible expression and tolerance. J Biochem Mol Toxicol 21, 289-98.

Lineweaver, H. and Burk, D., 1934. The Determination of Enzyme Dissociation Constants. Journal of the American Chemical Society 56, 658–666.

Livak, K.J. and Schmittgen, T.D., 2001. Analysis of relative gene expression data using real-time quantitative PCR and the 2(-Delta Delta C(T)) Method. Methods 25, 402-8.

Lu, S.C., 2013. Glutathione synthesis. Biochim Biophys Acta 1830, 3143-53.

Mannervik, B., Alin, P., Guthenberg, C., Jensson, H., Tahir, M.K., Warholm, M. and Jornvall, H., 1985. Identification of three classes of cytosolic glutathione transferase common to several mammalian species: correlation between structural data and enzymatic properties. Proc Natl Acad Sci U S A 82, 7202-6.

Mannervik, B. and Danielson, U.H., 1988. Glutathione transferases--structure and catalytic activity. CRC Crit Rev Biochem 23, 283-337.

Mitchell, P. and Tollervey, D., 2001. mRNA turnover. Curr Opin Cell Biol 13, 320-5.

Muthukumar, K. and Nachiappan, V., 2010. Cadmium-induced oxidative stress in Saccharomyces cerevisiae. Indian J Biochem Biophys 47, 383-7.

Nathaniel, C., Wallace, L.A., Burke, J. and Dirr, H.W., 2003. The role of an evolutionarily conserved cis-proline in the thioredoxin-like domain of human class Alpha glutathione transferase A1-1. Biochem J 372, 241-6.

Park, A.K., Moon, J.H., Jang, E.H., Park, H., Ahn, I.Y., Lee, K.S. and Chi, Y.M., 2013. The structure of a shellfish specific GST class glutathione S-transferase from antarctic bivalve Laternula elliptica reveals novel active site architecture. Proteins 81, 531-7.

Ramachandran, G.N., Ramakrishnan, C. and Sasisekharan, V., 1963. Stereochemistry of polypeptide chain configurations. J Mol Biol 7, 95-9.

Rhee, J.S., Lee, Y.M., Hwang, D.S., Won, E.J., Raisuddin, S., Shin, K.H. and Lee, J.S., 2007. Molecular cloning, expression, biochemical characteristics, and biomarker potential of theta class glutathione S-transferase (GST-T) from the polychaete Neanthes succinea. Aquat Toxicol 83, 104-15.

Rhee, J.S., Raisuddin, S., Hwang, D.S., Horiguchi, T., Cho, H.S. and Lee, J.S., 2008. A Mu-class glutathione S-transferase (GSTM) from the rock shell Thais clavigera. Comp Biochem Physiol C Toxicol Pharmacol 148, 195-203.

Ritchie, D.W., Kozakov, D. and Vajda, S., 2008. Accelerating and focusing protein-protein docking correlations using multi-dimensional rotational FFT generating functions. Bioinformatics 24, 1865-73.

Rossjohn, J., Board, P.G., Parker, M.W. and Wilce, M.C., 1996. A structurally derived consensus pattern for theta class glutathione transferases. Protein Eng 9, 327-32.

Rossjohn, J., McKinstry, W.J., Oakley, A.J., Verger, D., Flanagan, J., Chelvanayagam, G., Tan, K.L., Board, P.G. and Parker, M.W., 1998. Human theta class glutathione transferase: the crystal structure reveals a sulfate-binding pocket within a buried active site. Structure 6, 309-22.

Saranya Revathy, K., Umasuthan, N., Lee, Y., Choi, C.Y., Whang, I. and Lee, J., 2012. First molluscan theta-class Glutathione S-Transferase: identification, cloning, characterization and transcriptional analysis post immune challenges. Comp Biochem Physiol B Biochem Mol Biol 162, 10-23.

Schmuck, E.M., Board, P.G., Whitbread, A.K., Tetlow, N., Cavanaugh, J.A., Blackburn, A.C. and Masoumi, A., 2005. Characterization of the monomethylarsonate reductase and dehydroascorbate reductase activities of Omega class glutathione transferase variants: implications for arsenic metabolism and the age-at-onset of Alzheimer's and Parkinson's diseases. Pharmacogenet Genomics 15, 493-501.

Sheehan, D., Meade, G., Foley, V.M. and Dowd, C.A., 2001. Structure, function and evolution of glutathione transferases: implications for classification of non-mammalian members of an ancient enzyme superfamily. Biochem J 360, 1-16.

Singhal, S.S., Godley, B.F., Chandra, A., Pandya, U., Jin, G.F., Saini, M.K., Awasthi, S. and Awasthi, Y.C., 1999. Induction of glutathione S-transferase hGST 5.8 is an early response to oxidative stress in RPE cells. Invest Ophthalmol Vis Sci 40, 2652-9.

Stohs, S.J. and Bagchi, D., 1995. Oxidative mechanisms in the toxicity of metal ions. Free Radic Biol Med 18, 321-36.

Tahir, M.K., Guthenberg, C. and Mannervik, B., 1985. Inhibitors for distinction of three types of human glutathione transferase. FEBS Lett 181, 249-52.

Tamura, K., Stecher, G., Peterson, D., Filipski, A. and Kumar, S., 2013. MEGA6: Molecular Evolutionary Genetics Analysis version 6.0. Mol Biol Evol 30, 2725-9.

Tripathi, B.N. and Gaur, J.P., 2004. Relationship between copper- and zinc-induced oxidative stress and proline accumulation in Scenedesmus sp. Planta 219, 397-404.

Umasuthan, N., Revathy, K.S., Lee, Y., Whang, I., Choi, C.Y. and Lee, J., 2012. A novel molluscan sigma-like glutathione S-transferase from Manila clam, Ruditapes philippinarum: cloning, characterization and transcriptional profiling. Comp Biochem Physiol C Toxicol Pharmacol 155, 539-50.

Wallace, A.C., Laskowski, R.A. and Thornton, J.M., 1995. LIGPLOT: a program to generate schematic diagrams of protein-ligand interactions. Protein Eng 8, 127-34.

Wan, Q., Whang, I., Lee, J.S. and Lee, J., 2009. Novel omega glutathione S-transferases in disk abalone: Characterization and protective roles against environmental stress. Comp Biochem Physiol C Toxicol Pharmacol 150, 558-68.

Wilce, M.C., Board, P.G., Feil, S.C. and Parker, M.W., 1995. Crystal structure of a theta-class glutathione transferase. EMBO J 14, 2133-43.

Yamamoto, K., Zhang, P., Miake, F., Kashige, N., Aso, Y., Banno, Y. and Fujii, H., 2005. Cloning, expression and characterization of theta-class glutathione S-transferase from the silkworm, Bombyx mori. Comp Biochem Physiol B Biochem Mol Biol 141, 340-6.

Yang, Y., Cheng, J.Z., Singhal, S.S., Saini, M., Pandya, U., Awasthi, S. and Awasthi, Y.C., 2001. Role of glutathione S-transferases in protection against lipid peroxidation. Overexpression of hGSTA2-2 in K562 cells protects against hydrogen peroxide-induced apoptosis and inhibits JNK and caspase 3 activation. J Biol Chem 276, 19220-30.

Yu, Y., Liang, X.F., Li, L., He, S., Wen, Z.Y. and Shen, D., 2014. Two homologs of rho-class and polymorphism in alpha-class glutathione S-transferase genes in the liver of three tilapias. Ecotoxicol Environ Saf 101, 213-9.

ACKNOWLEDGMENT

There are so many people to thank for helping me during past two years. It would be so difficult to live in a totally different environment if they were not encouraging and accompanying during harsh moments in my short stay in South Korea.

First of all, I would like to convey my heartiest gratitude towards my academic supervisor, Professor Jehee Lee for his enormous support and guidance to make this a success. It was a great honor and pleasure to be a member of his Marine Molecular Genetics Laboratory (MMGL). His valuable insights and assessments helped me to upgrade myself academically and professionally. Secondly, I would like to express my gratitude to the thesis Director Dr. Qiang Wan and Assistant Professor Chulhong Oh who evaluated my thesis. Their encouragement and suggestions were valuable to me in leaps and bounds to improve my study.

I would also like to convey my sincere gratitude to Mr. J.K.T.P. Jayasooriya and Dr. W.D.N. Wickramaarachchi who introduced and recommended me to Professor Jehee Lee. I would acknowledge Mr. S.D.N.K. Bathige who supported me during entire research period in all the ways. Without him this achievement would be just a dream to me. I thankful to Dr. Qiang Wan again for his guidance and encouragement he owed me during research work in MMGL. His support made me more polished and independent when handling a research project. My sincere gratitude goes to Mr. D.A.S. Elvitigala who guided me and helped me to achieve my research goals. I would also like to acknowledge Mr. G.I. Godahewa who introduced me the laboratory ethics and the basic laboratory skills practiced in the laboratory.

I extend my sincere thanks to my heartier friends; Ms Eunyoung and Ms Jiyeon who supported me during two years stay in MMGL. I would also like to thank all my other MMGL and Hamdeok laboratory members, Dr. Hwang, Dr. Jung, Dr. Lim, Dr. Jin, Dr. Umasuthan, Ms. Sukkyoung, Mr. Yucheol, Mrs. Thulasitha, Mr. Thiunuwan, Ms. Minyoung, Mr. Seongdo, Mr. Viraj, Mr. Lalinka, Ms. Mothishri, Ms. Jeongin, Ms. Sunhye, Ms. Gabin, Mrs. Nadeesahni, Mr. Sachith, Mr. Kugapreethan Ms. Jeongeun and Ms. Hyowon. Again I would like to thank all the Sri Lankan members in Jeju National University (JNU), Mr. Buddhi, Mr. Susara, Mrs. Dilshara, Mrs. Hamsanandini, Mr. Lakmal, Mr. Malintha, Mr. Madusahn, Mr. Shanura, Mr. Asanka and Mrs. Madhushani.

I would like to dedicate my research work to my loving parents and my sister for their unflagging love and support. Without them nothing is possible in my life.